HEAPS OF RHOMBIC DODECAHEDRA, CATALAN CONGRUENCES ON ALTERNATING SIGN MATRICES, AND BASES OF THE TEMPERLEY–LIEB ALGEBRA

FLORENT HIVERT, VINCENT PILAUD, AND LUDOVIC SCHWOB

Abstract. We prove that the excedance relation on permutations defined by N. Bergeron and L. Gagnon actually extends to a congruence of the lattice on alternating sign matrices. Motivated by this example, we study all lattice congruences of the lattice on alternating sign matrices whose quotient is isomorphic to the Stanley lattice on Dyck paths, which we call catalan congruences. We prove that the maxima of the congruence classes are always covexillary permutations (and all covexillary permutations appear this way), and that the minimal permutations in each class are always precisely the 321-avoiding permutations. Finally, we show that any choice of representative permutations in each congruence class yield a basis of the Temperley–Lieb algebra with parameter 2, vastly generalizing the bases arising from the excedance relation.

Contents

VP was partially supported by the Spanish project PID2022-137283NB-C21 of MCIN/AEI/10.13039/501100011033 / FEDER, UE, by the Spanish–German project COMPOTE (AEI PCI2024-155081-2 & DFG 541393733), by the Severo Ochoa and María de Maeztu Program for Centers and Units of Excellence in R&D (CEX2020-001084-M), by the Departament de Recerca i Universitats de la Generalitat de Catalunya (2021 SGR 00697), and by the French–Austrian project PAGCAP (ANR-21-CE48-0020 & FWF I 5788).

1. Introduction

It is well known that the quotient $\mathbf{K}[X]/\langle \mathrm{Sym}^+(X)\rangle$ of the polynomial ring on an alphabet $X = \{x_1, \dots, x_n\}$ of n variables by the ideal generated by symmetric polynomials with no constant terms is of dimension $n!$ and is isomorphic to the regular representation of the symmetric group $\mathfrak{S}_n$. Chevalley–Shephard–Todd's theorem asserts that this statement remains true when the symmetric group is replaced by any real or complex reflection group. In the combinatorics community, a large body of work has been devoted to understanding this representation-theoretic structure in more explicit terms. One notable outcome is A. Lascoux's theory of Schubert polynomials [LS87, Mac91], which provides a remarkably elegant basis for the above quotient. This perspective also connects to the celebrated $n!$ conjecture [GH93, Hai01], which extends the setting from one set of variables to two alphabets and gives rise to deep interactions between algebraic geometry, representation theory, and combinatorics.

There is another closely related case which, however, remains much less understood: the ring of quasi-symmetric polynomials. Recall that these were introduced by I. Gessel [Ges84] as generating series encoding permutations with a prescribed descent set. While many parallels with the theory of symmetric functions have been developed, both from combinatorial and representation-theoretic perspectives [KT97, Hiv00], the invariant-theoretic viewpoint has long remained elusive. Nevertheless, there have been persistent indications that a structure analogous to the symmetric and coinvariant settings should exist.

On one hand, the first author proved that the ring of quasi-symmetric polynomials is invariant under a modified action of the symmetric group [Hiv00]. In contrast to the classical situation, this action is not faithful and factors through the Temperley–Lieb algebra TL(2), whose dimension is the n-th Catalan number C_n. On the other hand, J. C. Aval and N. Bergeron [AB03] noticed that the quotient $\mathbf{K}[X]/\langle \mathrm{QSym}^+(X)\rangle$ is also of dimension C_n. However, the connection between these two occurrences of Catalan numbers is far from straightforward. The reason is that the Temperley–Lieb action is not multiplicative, and therefore does not descend to the quotient. As a result, the space $\mathbf{K}[X]/\langle \mathrm{QSym}^+(X)\rangle$ does not naturally inherit an action of TL(2), making the relationship between the two Catalan structures subtle to uncover.

In a recent breakthrough [BG24], N. Bergeron and L. Gagnon constructed a particular set of C_n permutations whose projection in TL(2) gives a basis, and such that the graded ideal of the vanishing ideal is equal to $\langle \mathrm{QSym}^+(X)\rangle$. More precisely, they defined the *excedance equivalence* $\equiv$ on permutations of $[n]$, where two permutations are excedance equivalent if they share the same sets of positions and of values of their excedances (see Definition 3.1 and Figure 11). We summarize their main results into the following statement.

Theorem 1.1 ([BG24]). *For the excedance relation on permutations,*

(i) the excedance classes are intervals of the Bruhat order, whose minimal elements are precisely the 321*-avoiding permutations, and whose maximal elements are some covexillary permutations already considered in* [Zin02, GW16]*,*
(ii) the poset quotient of the (strong) Bruhat order on permutations by the excedance relation is isomorphic to the Stanley lattice on Dyck paths,
(iii) any choice of representatives of the excedance classes yields a basis of the Temperley–Lieb algebra TL(2)*,*
(iv) the top degree homogeneous components of the vanishing ideal of the set of permutations which are maximal in their excedance classes and the positive degree quasisymmetric polynomials generate the same ideal.

Our work starts from the observation that this excedance relation on the Bruhat order actually extends to a congruence of the lattice of alternating sign matrices (which is the MacNeille completion of the Bruhat order). The congruences of a lattice are the equivalence relations which respect the lattice structure, and they come with rich combinatorial and algebraic properties. Our main results (partially) extend the results of [BG24] to all lattice congruences $\equiv$ on alternating sign matrices whose quotient is isomorphic to the Stanley lattice, which we call *catalan congruences*.

Theorem 1.2. *For any catalan congruence $\equiv$ of the lattice of alternating sign matrices,*

(i) the maximal alternating sign matrices of the congruence classes of $\equiv$ are covexillary permutation matrices,
(ii) the minimal permutation matrices in the congruence classes of $\equiv$ are precisely the 321*-avoiding permutation matrices,*
(iii) any choice of representative permutation matrices in each congruence class of $\equiv$ yields a basis of the Temperley–Lieb algebra.

A few comments on this statement. In (i), the covexillary permutation matrices that appear as maxima of congruence classes depend on the congruence. However, any covexillary permutation matrix appears as the maxima of a class for at least one catalan congruence. In (ii), the minimal alternating sign matrix of each class is not necessarily a permutation (we actually discuss along the paper the specific congruences with this property). But the permutations in each congruence class form an interval of the Bruhat order, whose minimum is 321-avoiding and whose maximum is covexillary, and (by counting) all 321 permutations appear as minimal permutations of congruence classes. Finally, we note that the problem to extend Theorem 1.1 (iv) to any catalan congruence will be investigated in a future paper.

Our approach to Theorem 1.2 is a combination of lattice and geometric perspectives on alternating sign matrices. It is well known that the lattice of alternating sign matrices is distributive, hence isomorphic to the inclusion lattice of lower sets of its join irreducible subposet by the fundamental theorem for distributive lattices. As already observed and exploited in [Pro01, Str11], the join irreducible poset of the lattice of alternating sign matrices can be seen geometrically as a poset on the integer points inside the $(n-2)$th dilate of a 3-dimensional tetrahedron resting on an edge (see Figure 3). Pushing slightly further this geometric perspective in Section 2.3, we interpret a lower set in this tetrahedral poset as a stack of rhombic tetrahedra (see Figure 8). The upper hull of this stack is the colored polygonal surface separating the lower set from its complementary upper set (see Figure 5). Projecting this surface to the ground (see Figure 6) naturally leads to interpret geometrically the classical combinatorial models in bijection with alternating sign matrices (*e.g.* height functions, six-vertex model, fully packed loop), and to cook up some seemingly new models (*e.g.* cliff model). We note that this perspective also naturally leads to higher dimensional analogues of alternating matrices which will deserve further investigation.

The quotients of a distributive lattice $\mathbf{L}$ are distributive lattices, whose join irreducible posets are induced subposets of the join irreducible poset of $\mathbf{L}$. Understanding quotients of the lattice of alternating sign matrices isomorphic to the Stanley lattice on Dyck paths thus boils down to finding subposets of the tetrahedron poset isomorphic to the triangular poset. Simple geometric arguments show that these triangular subposets of the tetrahedron are encoded by certain depth triangles (see Section 4.3), which are in natural bijections with doubly gapless Gelfand–Tsetlin patterns with bottom row $12\dots(n-1)$ (see Section 4.4), and with bicolored pipe dreams with $n-2$ pipes (see Section 4.5). Interestingly, these depth triangles are themselves endowed with a natural lattice structure (see Figure 23), which we exploit to show Theorem 1.2 in Sections 5, 6 and 7.

Finally, we introduce in Section 8 a general operation of symmetrization of posets which specializes to the join irreducible posets of the lattices considered in this paper. We show in particular that the poset resulting of this symmetrization can be described by inequalities indexed by upper sets of the original poset.

2. Two distributive lattices

2.1. **Meet and join representations in distributive lattices.** We first recall some classical facts about distributive lattices. A *lower* (resp. *upper*) *set* of a poset $\mathcal{P}$ is a subset X of $\mathcal{P}$ such that $x \in X$ and $x \geq y$ (resp. $x \leq y$) implies $y \in X$. A *lattice* $\mathbf{L}$ is a poset where any two elements $x, y \in \mathbf{L}$ admits a *join* $x \vee y$ (least upper bound) and a *meet* $x \wedge y$ (greatest lower bound). It is *distributive* if $x \vee (y \wedge z) = (x \vee y) \wedge (x \vee z)$ and $x \wedge (y \vee z) = (x \wedge y) \vee (x \wedge z)$ for all $x, y, z \in \mathbf{L}$ (in fact, these two conditions are equivalent). An element $x \in \mathbf{L}$ is *join* (resp. *meet*) *irreducible* if it covers (resp. is covered by) a single element $x_\star$ (resp. $x^\star$). We denote by $\mathcal{J}(\mathbf{L})$ (resp. $\mathcal{M}(\mathbf{L})$) the subposet of $\mathbf{L}$ induced by its join (resp. meet) irreducible elements. The following classical result is known as the fundamental theorem for distributive lattices.

Theorem 2.1 (Birkhoff)**.**

- *The set* $\mathbf{Lo}(\mathcal{P})$ *(resp.* $\mathbf{Up}(\mathcal{P})$*) of lower (resp. upper) sets of any poset* $\mathcal{P}$ *ordered by inclusion forms a distributive lattice.*
- *Conversely, any distributive lattice* $\mathbf{L}$ *is isomorphic to the inclusion poset of lower (resp. upper) sets of its join (resp. meet) irreducible poset* $\mathcal{J}(\mathbf{L})$ *(resp.* $\mathcal{M}(\mathbf{L})$*).*

For $x \in \mathbf{L}$, we denote by $\mathrm{J}(x) := \{j \in \mathcal{J}(\mathbf{L}) \mid j \leq x\}$ the corresponding lower set of $\mathcal{J}(\mathbf{L})$, and by $\mathrm{j}(x) := \max(\mathrm{J}(x))$ the corresponding antichain of $\mathcal{J}(\mathbf{L})$. We define dually $\mathrm{M}(x) := \{m \in \mathcal{M}(\mathbf{L}) \mid x \leq m\}$ and $\mathrm{m}(x) := \min(\mathrm{M}(x))$.

Note that there is a canonical isomorphism between the posets $\mathcal{J}(\mathbf{L})$ and $\mathcal{M}(\mathbf{L})$ defined by $\kappa(j) = \bigvee \{x \in \mathbf{L} \mid x \wedge j = j_\star\}$. It has the property that $\mathrm{M}(x) = \kappa(\mathcal{J}(\mathbf{L}) \smallsetminus \mathrm{J}(x))$. In other words, an element of $\mathbf{L}$ can be thought of as a *cut* separating a lower set from an upper set in the poset $\mathcal{J}(\mathbf{L}) \simeq \mathcal{M}(\mathbf{L})$,

For instance, the chain with $n+1$ elements is (isomorphic to) the lattice of lower (resp. upper) sets of a chain $1 - 2 - \cdots - n$, and the map κ is given by $\kappa(i) = i - 1$.

2.2. **Dyck paths.** A *Dyck path* of semilength n is a path with up steps $(1, 1)$ and down steps $(1, -1)$, starting at $(0, 0)$, ending at (n, n), and never passing strictly below the horizontal axis. They define the *Dyck path lattice* $\mathbf{Dyck}_n$ (also known as the *Stanley lattice*) with the relation $P \leq Q$ if P stays below Q. See Figure 2 (left). The join (resp. meet) irreducible Dyck paths are those with a single peak (resp. valley), hence the poset $\mathcal{J}(\mathbf{Dyck}_n)$ (resp. $\mathcal{M}(\mathbf{Dyck}_n)$) is isomorphic to the triangular poset $\mathcal{D}_n$ of triples (y_1, y_2, y_3) with $y_1 + y_2 + y_3 = n - 2$, ordered by $(y_1, y_2, y_3) \leq (z_1, z_2, z_3)$ if and only if $y_1 + y_2 \leq z_1 + z_2$ and $y_2 + y_3 \leq z_2 + z_3$. See Figure 3 (left). (Note that this poset could be encoded using two coordinates. However, we prefer to work with barycentric coordinates throughout the paper, as they make the presentation more symmetric.)

2.3. **Alternating sign matrices.** We closely follow the presentation of [Pro01]. For $n \geq 1$, one can define three families of matrices, illustrated in Figure 4:

- An *alternating sign matrix* (ASM) of order n is an $(n \times n)$-matrix $A = (A_{i,j})_{i,j \in [n]}$ with entries -1, 0 or 1, with row and column sums equal to 1, and such that nonzero entries alternate between 1 and -1 in each row and each column.

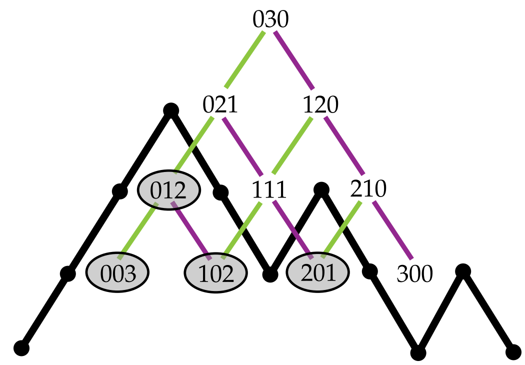

FIGURE 1. A lower set of $\mathcal{D}_5$ and the corresponding Dyck path of semilength 5.

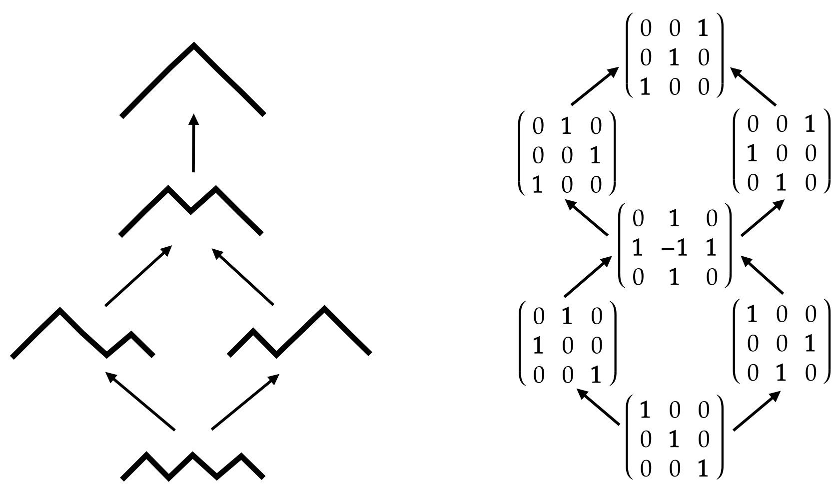

FIGURE 2. The Stanley lattice $\mathbf{Dyck}_3$ (left) and the ASM lattice $\mathbf{ASM}_3$ (right).

- A *corner sum matrix* (CSM) of order n is an $(n+1) \times (n+1)$-matrix whose first row and column consist of 0 and last row and column consist of the numbers from 0 to n in increasing order, and each entry is either equal to, or one more than the preceding entry in its row and in its column.
- A *height function matrix* (HFM) of order n is an $(n+1) \times (n+1)$-matrix whose first (resp. last) row and column consist of the numbers from 0 to n in increasing (resp. decreasing) order, and any two consecutive entries in a row or a column differ by 1.

As illustrated in Figure 4, there are simple bijections between these families of matrices:

- the CSM C of an ASM A is defined by $C_{i,j} = \sum_{i' \le i, j' \le j} A_{i',j'}$ for $0 \le i, j \le n$,
- the HFM H of a CSM C is defined by $H_{i,j} = i + j - 2C_{i,j}$ for $0 \le i, j \le n$.

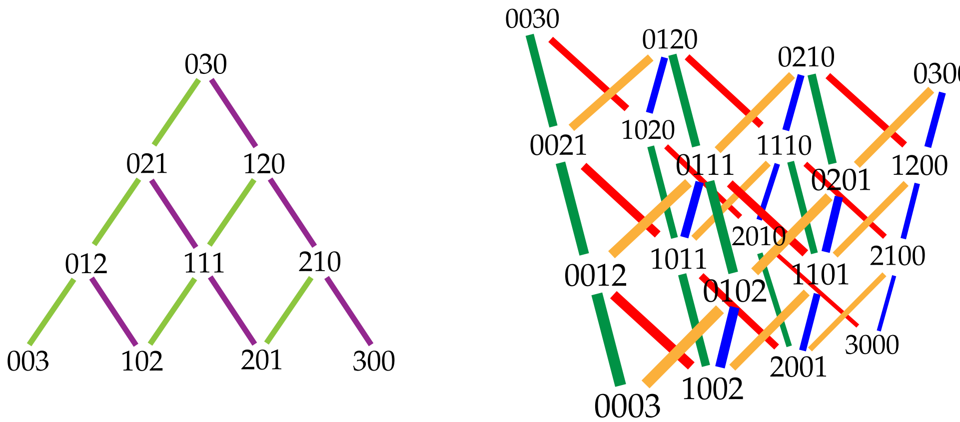

FIGURE 3. The posets $\mathcal{D}_5$ (left) and $\mathcal{T}_5$ (right).

$$\begin{pmatrix} \cdot & \cdot & + & \cdot & \cdot \\ \cdot & + & - & + & \cdot \\ \cdot & \cdot & + & - & + \\ + & - & \cdot & + & \cdot \\ \cdot & + & \cdot & \cdot & \cdot \end{pmatrix} \quad \begin{pmatrix} 0 & 0 & 0 & 0 & 0 & 0 \\ 0 & 0 & 0 & 1 & 1 & 1 \\ 0 & 0 & 1 & 1 & 2 & 2 \\ 0 & 0 & 1 & 2 & 2 & 3 \\ 0 & 1 & 1 & 2 & 3 & 4 \\ 0 & 1 & 2 & 3 & 4 & 5 \end{pmatrix} \quad \begin{pmatrix} 0 & 1 & 2 & 3 & 4 & 5 \\ 1 & 2 & 3 & 2 & 3 & 4 \\ 2 & 3 & 2 & 3 & 2 & 3 \\ 3 & 4 & 3 & 2 & 3 & 2 \\ 4 & 3 & 4 & 3 & 2 & 1 \\ 5 & 4 & 3 & 2 & 1 & 0 \end{pmatrix}$$

FIGURE 4. An ASM, a CSM, and a HFM, all corresponding to each other.

(Note that we label the rows and columns of ASMs from 1 to n and the rows and columns of CSMs and HFMs from 0 to n.)

The HFMs of order n ordered by entrywise comparison define a distributive lattice $\mathbf{HFM}_n$ where the join (resp. meet) of two HFMs H and H' is the HFM with (i,j)-entry $\max(H_{i,j}, H'_{i,j})$ (resp. $\min(H_{i,j}, H'_{i,j})$). Note that two HFMs $H, H' \in \mathbf{HFM}_n$ form a cover relation $H \lessdot H'$ if and only if there is $0 < i, j < n$ such that $H'_{i,j} = H_{i,j} + 2$ and $H'_{k,\ell} = H_{k,\ell}$ for all $0 < k, \ell < n$ with $(i,j) \neq (k,\ell)$. We then say that (i,j) is an *ascent* of H and a *descent* of H'.

We now introduce a geometric interpretation of the join irreducible poset following [Pro01, Str11]. The join irreducible poset $\mathcal{J}(\mathbf{HFM}_n)$ can be seen geometrically as a poset $\mathcal{T}_n$ on the integer points inside the $(n-2)$th dilate of a 3-dimensional tetrahedron resting on an edge [Pro01]. See Figure 3. Namely, using barycentric coordinates, this poset is defined on the quadruples $\boldsymbol{x} := (x_1, x_2, x_3, x_4) \in \mathbb{N}^4$ with $x_i \geq 0$ for $i \in [4]$ and $x_1 + x_2 + x_3 + x_4 = n-2$ ordered by $\boldsymbol{x} \leq \boldsymbol{y}$ if and only if $x_1 \geq y_1$, $x_2 \leq y_2$, $x_3 \leq y_3$ and $x_4 \geq y_4$. Its cover relations are the pairs $\boldsymbol{x} \lessdot \boldsymbol{y}$ such that $\boldsymbol{y} - \boldsymbol{x}$ is one of the four vectors $b := (-1, 1, 0, 0)$, $r := (-1, 0, 1, 0)$, $o := (0, 1, 0, -1)$ and $g := (0, 0, 1, -1)$. We draw these vectors in 4 distinct colors, blue, red, orange, green. We can thus see an HFM as a lower set in this 4-colored tetrahedral poset, as illustrated in Figure 5 (left).

Note that via the above-mentioned bijection between ASMs and HFMs, we can transport the lattice $\mathbf{HFM}_n$ on HFMs of order n to a lattice $\mathbf{ASM}_n$ on ASMs of order n. See

Figure 2 (right). This lattice is the MacNeille completion of the Bruhat order on permutations of $[n]$. We call *ascents* and *descents* of an ASM the ascents and descents of its corresponding HFM. The join (resp. meet) irreducible ASMs are known to be the matrices of the *bigrassmannian* (resp. *anti-bigrassmannian*) permutations, *i.e.* the permutations σ such that σ and its inverse σ^{-1} have only one descent (resp. ascent). Namely, an integer point $\boldsymbol{x} = (x_1, x_2, x_3, x_4)$ in the tetrahedron corresponds to the bigrassmannian and anti-bigrassmannian permutations

$$j(\boldsymbol{x}) = \begin{pmatrix} I_{x_1} & 0 & 0 & 0 \\ 0 & 0 & I_{x_2+1} & 0 \\ 0 & I_{x_3+1} & 0 & 0 \\ 0 & 0 & 0 & I_{x_4} \end{pmatrix} \qquad \text{and} \qquad m(\boldsymbol{x}) = \begin{pmatrix} 0 & 0 & 0 & \bar{I}_{x_2} \\ 0 & \bar{I}_{x_1+1} & 0 & 0 \\ 0 & 0 & \bar{I}_{x_4+1} & 0 \\ \bar{I}_{x_3} & 0 & 0 & 0 \end{pmatrix}$$

where I_k (resp. $\bar{I}_k$) is the $k \times k$ identity (resp. anti-identity) matrix with 1 on the diagonal (resp. anti-diagonal) and 0 everywhere else.

It is also interesting to represent an ASM as the surface S separating the lower set X of $\mathcal{T}_n$ and its complement. For this, we include additional edges so that each integer point of the tetrahedron gets 12 incident arrows (one in the direction $\boldsymbol{e}_i - \boldsymbol{e}_j$ for each $i \neq j \in [4]$). The horizontal edges, in direction $\pm(1, 0, 0, -1)$ and $\pm(0, 1, -1, 0)$, are colored in gray. The additional endpoints are considered in X (resp. in its complement) if they are incident to an arrow which is also incident to one of the two bottom (resp. top) faces of the tetrahedron. We then add a rhombus orthogonal to each arrow from a point in X to a point in its complement (the color of the rhombus matches the color of the orthogonal arrow). The corresponding surface is illustrated in Figure 5 (middle and right).

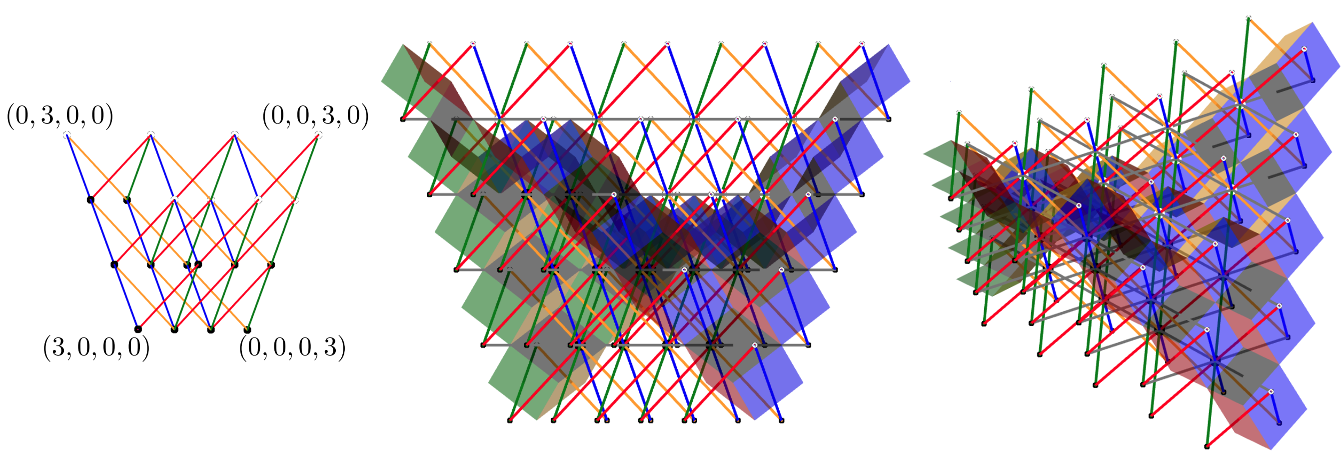

FIGURE 5. The ASM of Figure 4 seen as a lower set X of the tetrahedron poset $\mathcal{T}_5$ (left) or equivalently as the surface separating X from its complement (middle and right).

As illustrated in Figure 6, looking at this surface S from above (meaning in the direction $(-1, 1, 1, -1)$, or more precisely under the projection $(x_1, x_2, x_3, x_4) \mapsto (x_1 + x_2, x_1 + x_3)$) makes transparent some well-known bijections between classical equivalent combinatorial models for ASMs (and naturally motivates combinatorial models that were not considered before to the best of our knowledge):

- Seen from above, the colored rhombi of S forms a *rainbow tiling*. See Figure 6 (a). The tiled zone is formed by n rows and n columns of $n+1$ tiles each. Hence, we have $2n(n+1)$ tiles in total. We call *integer points* the vertices in the middle of a row and a column (see Figure 6 (c)), and *half integer points* the other vertices (see Figure 6 (d)). A rainbow tiling is a 4-coloring of the tiles such that
  - the south/east/north/west tiles are colored red/blue/orange/green,
  - the rows (resp. columns) are colored with cold colors blue/green (resp. with warm colors red/orange),
  - each integer point sees either 2 or 4 colors.

  Note that, up to recoloring, this rainbow tiling is equivalent to a 4-coloring of the *aztec diamond*.
- The *ASM* records the saddle points of S, seen from above. Namely, the $+1$ and -1 of the ASM are the two types of saddle points of S (depending on the orientation of the principal directions of the saddle point). They can be visualized as the rainbow integer points (*i.e.* surrounded by the four colors red/blue/orange/green) of the rainbow tiling of Figure 6 (a). See Figure 6 (b).
- The *six-vertex model* is given by the horizontal diagonals of the rhombi of S, oriented counterclockwise around the surface S (in other words, in the direction of the march of the dahu[1]), and seen from above. See Figure 6 (c). Equivalently, it can be obtained by placing south/west/north/east pointing arrows in the red/blue/orange/green tiles of the rainbow tiling of Figure 6 (a). This gives an orientation of the integer grid such that
  - the extremal horizontal (resp. vertical) arrows are incoming (resp. outgoing),
  - each integer point has two incoming and two outgoing arrows.

  It is called six-vertex model as it has 6 types of vertices: .
  Note that, as the nonzero entries of the ASM correspond to saddle points of S, they correspond to the vertices of the six-vertex model with opposite incoming arrows and opposite outgoing arrows. See the connection between Figure 6 (b) & (c).
- The *six-square model* is given by the non-horizontal diagonals of the rhombi of S, oriented upwards, and seen from above. See Figure 6 (d). Equivalently, it can be obtained by placing east/south/west/north pointing arrows in the red/blue/orange/green tiles of the rainbow tiling of Figure 6 (a). Equivalently, it is the dual directed graph of the six-vertex model of Figure 6 (c) (meaning that each arrow is rotated by 90°). This gives an orientation of the half-integer grid such that
  - the arrows on the bottom/right/top/left side are oriented east/south/west/north,
  - each mesh, traveled clockwise, has two forward and two backward arrows.

  We call it six-square model as there are 6 types of squares: .

[1]https://en.wikipedia.org/wiki/Dahu

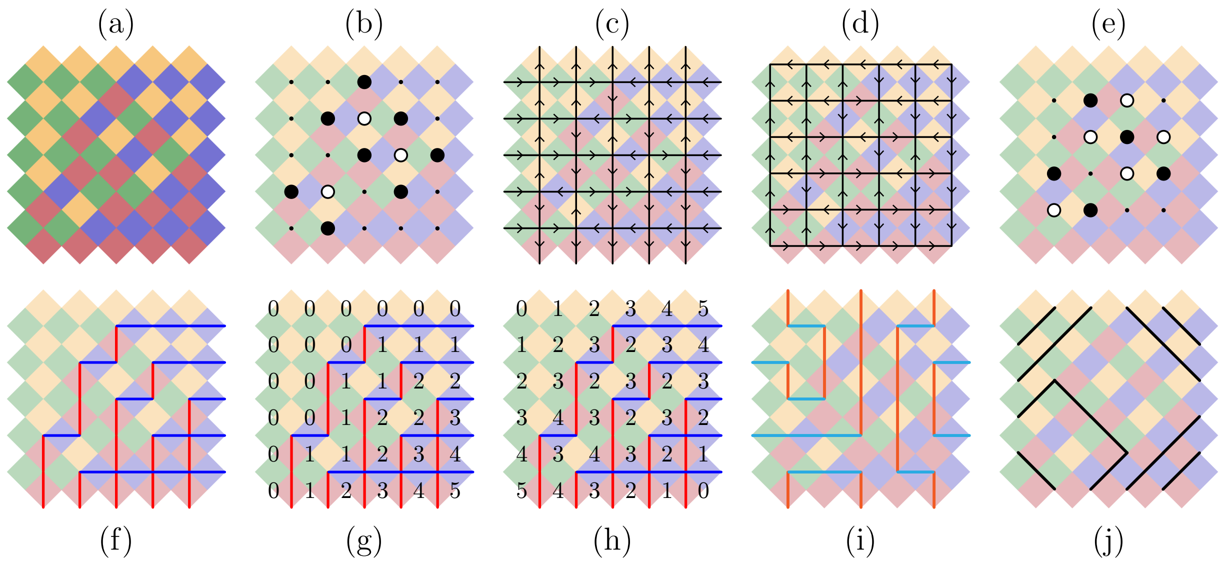

Figure 6. Reading bijections on the surface of the ASM of Figure 4.

- The *peak–pit matrix* is given by the local optima of the surface S, seen from above. Figure 6 (e). They can be visualized as the rainbow half integer points of the rainbow tiling of Figure 6 (a). Equivalently, they are the points with indegree or outdegree 4 in the six-square model of Figure 6 (d). We are not aware that this model has been studied before.
- The *six-vertex configuration* is given by the horizontal diagonals of the red and blue rhombi of S, seen from above. See Figure 6 (f). Equivalently, they are the east and south pointing arrows in the six-vertex model of Figure 6 (c). They correspond to distinct adjacent entries in the CSM (see Figure 6 (g)) and to decreasing adjacent entries in the HFM (see Figure 6 (h)).
- The *HFM* records the height of the surface above each integer point seen from above. See Figure 6 (h).
- The *fully packed loop* is given by the horizontal diagonals of the red and orange (resp. green and blue) rhombi of S located at odd (resp. even) heights, seen from above. See Figure 6 (e).
- The *cliffs configuration* is given by the cliffs (gray rhombi) of S, seen from above. See Figure 6 (f). Equivalently, it is obtained from the HFM by joining the two equal heights in each (2×2)-submatrix containing 3 distinct heights. Cliffs configurations are exactly the configurations of paths where each point inside a square grid belongs to an even number of diagonal steps (0, 2 or 4), and points on the border belong to one diagonal step and are connected to points of the same height. We are not aware that this model has been studied before.

Figure 7 illustrates these correspondence on bigger examples of ASM (b), peak-pit model (e), fully packed loop (i), and cliff model (j).

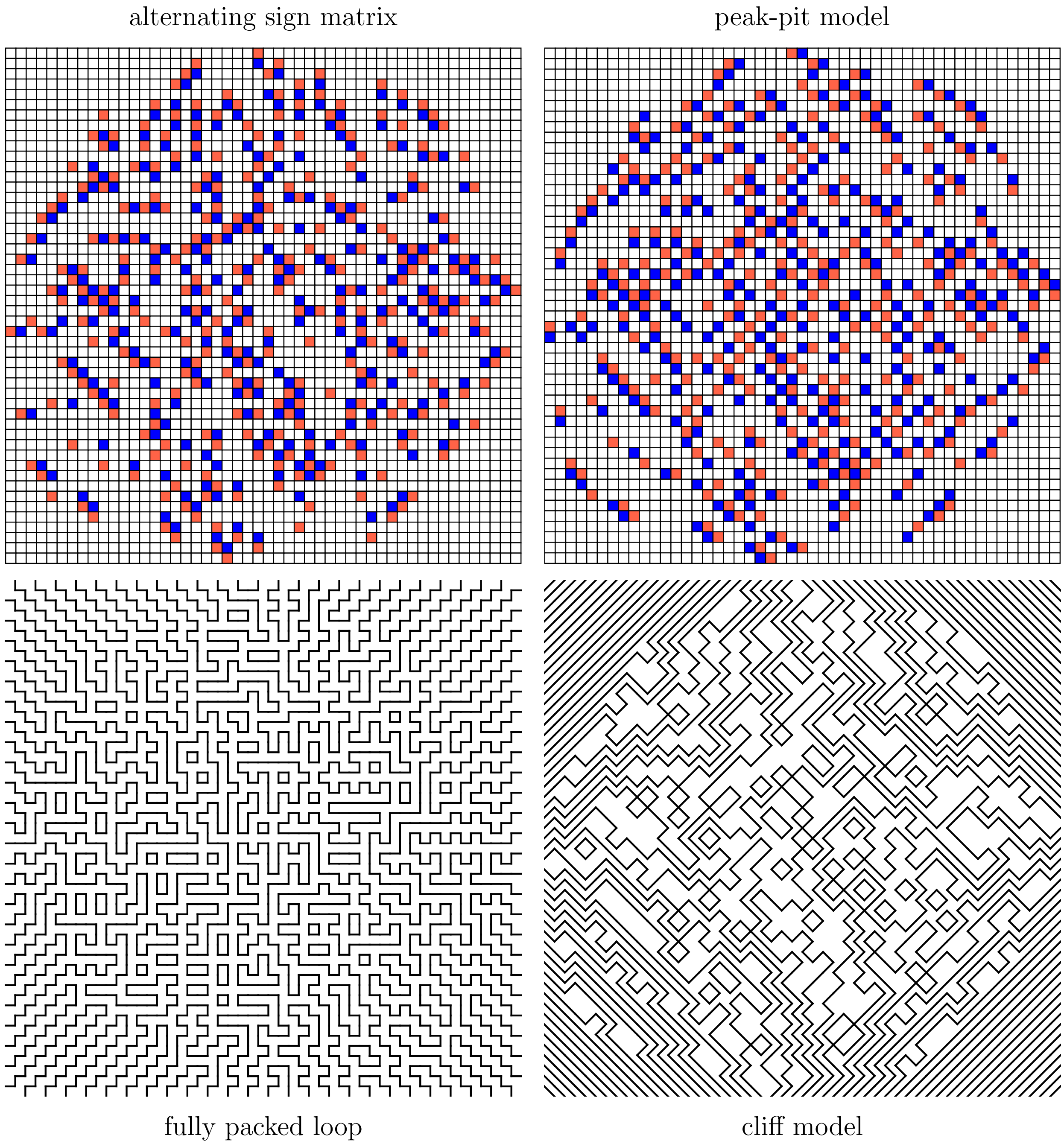

Figure 7. Bigger examples of the correspondence between ASM, peak-pit model, fully packed loop, and cliff model.

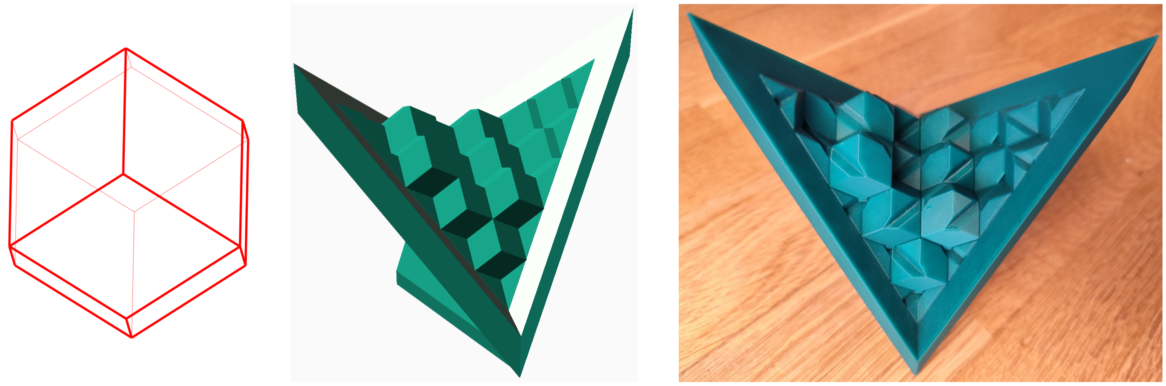

FIGURE 8. The rhombic dodecahedron (left), and the ASM of Figure 4 seen as a pile of rhombic dodecahedra, as 3d objects in OpenSCAD (middle) and in real life (right).

Finally, it is also interesting to represent an ASM as a stack of rhombic dodecahedra. Remember that the *rhombic dodecahedron* is the polytope obtained

- either as the convex hull of the 8 vertices $\pm\boldsymbol{e}_1\pm\boldsymbol{e}_2\pm\boldsymbol{e}_3$ of the standard cube together with the 6 points $\pm 2\boldsymbol{e}_i$ for $i \in [3]$,
- or as the intersection of the 12 halfspaces defined by $\langle \boldsymbol{r} | \boldsymbol{x} \rangle \le 1$ for the roots $\boldsymbol{r}$ of type A_3.

See Figure 8 (left). It is precisely the Voronoi cell of the integer point lattice generated by the root system of type A_3. Hence, we can see a lower set X of the tetrahedron poset as a stack of rhombic dodecahedra. The advantage of this model is that it can be 3d-printed and manipulated (see Figure 8), after adding a suitable support (containing the rhombic dodecahedra corresponding to the points added to X above). The surface S discussed above is the upper boundary of this stacking (including the additional rhombic dodecahedra of the support).

2.4. **Higher dimensional analogues.** It is of course tempting to consider higher dimensional analogues of Sections 2.2 and 2.3. Fix three integers d, k, n and consider the poset $P(d, k, n)$ whose

- elements are the integer points in the $(n-2)$th dilate of the d-dimensional simplex embedded in the standard way in $\mathbb{R}^{d+1}$,
- cover relations are pairs of points $(\boldsymbol{x}, \boldsymbol{y})$ such that $\boldsymbol{x} - \boldsymbol{y} = \boldsymbol{e}_i - \boldsymbol{e}_j$ with $i \le k < j$.

Let $Q(d, k, n)$ denote the distributive lattice of lower sets of $P(d, k, n)$. For example, $Q(2, 2, n)$ is the Stanley lattice, and $Q(3, 2, n)$ is the ASM lattice.

The Voronoi cell of the integer point lattice generated by the root system of type A_d is the graphical zonotope $Z(d)$ of a $(d+1)$-cycle. This is a polytope with $2 \times (2^d - 1)$ vertices (corresponding to all the acyclic orientations of the $(d+1)$-cycle) and $2 \times \binom{d+1}{2}$ facets (corresponding to the biconnected subsets of the $(d+1)$-cycle). For $d = 3$, it is the rhombic dodecahedron with 14 vertices and 12 facets illustrated in Figure 8. We can thus see an element of $D(d,k,n)$ as a stacking of copies of $Z(d)$.

Now, one can try to understand the other models for ASMs in this framework. More precisely, given an element of $Q(d,k,n)$, *i.e.* a stacking of copies of $Z(d)$, we can look at it from the direction $\boldsymbol{w} = (\boldsymbol{e}_1 + \ldots + \boldsymbol{e}_k) - (\boldsymbol{e}_{k+1} + \ldots + \boldsymbol{e}_{d+1})$ and try to encode it by the following models:

- remembering the height above each point, seen from the direction $\boldsymbol{\omega}$,
- remembering the colors (*i.e.* directions) of the upper faces of the stacking, seen from the direction $\boldsymbol{\omega}$,
- remembering the saddle points of the stacking, more precisely their types (1 or -1) and positions under the projection in direction $\boldsymbol{w}$,
- remembering the peaks and pits of the stacking, seen from the direction $\boldsymbol{w}$,
- remembering the cliffs of the stacking, seen from the direction $\boldsymbol{\omega}$.

When the dimension is too small ($d = 1$ and sometimes for $d = 2$), some of these models are not rich enough to recover the stacking (in particular the saddle point model). But as soon as the dimension is at least $d = 3$, all these models allow one to encode the stackings. This yields interesting generalizations of Dyck paths and ASMs that deserve further study.

3. The excedance congruence of $\mathbf{ASM}_n$

This section defines a relevant lattice congruence of $\mathbf{ASM}_n$, extending the excedance relation of the Bruhat order on permutations defined by N. Bergeron and L. Gagnon in [BG24].

3.1. Lattice morphisms and congruences.

A *lattice morphism* is a map $\phi : \mathbf{L} \to \mathbf{K}$ between two lattices which respects meets and joins, *i.e.* such that $\phi(x \vee y) = \phi(x) \vee \phi(y)$ and $\phi(x \wedge y) = \phi(x) \wedge \phi(y)$ for any $x, y \in \mathbf{L}$. A *congruence* of a lattice $\mathbf{L}$ is an equivalence relation $\equiv$ on $\mathbf{L}$ which respects meets and joins, *i.e.* $x \equiv x'$ and $y \equiv y'$ implies $x \vee y \equiv x' \vee y'$ and $x \wedge y \equiv x' \wedge y'$ for any $x, y \in \mathbf{L}$. The *quotient* $\mathbf{L}/{\equiv}$ is the lattice on the equivalence classes of $\mathbf{L}$ where

- $X \le Y$ if and only if there exist $x \in X$ and $y \in Y$ such that $x \le y$,
- $X \vee Y$ (resp. $X \wedge Y$) is the equivalence class of $x \vee y$ (resp. $x \wedge y$) for any representatives $x \in X$ and $y \in Y$.

Note that the equivalence classes of a congruence are always intervals of $\mathbf{L}$, and that the quotient $\mathbf{L}/{\equiv}$ is isomorphic (as poset) to the subposet of $\mathbf{L}$ induced by the minimal (resp. maximal) elements of the congruence classes. Observe also that

- the projection map $\mathbf{L} \to \mathbf{L}/{\equiv}$ of a congruence $\equiv$ on $\mathbf{L}$ is a surjective lattice morphism,
- conversely, the fibers of a surjective lattice morphism $\mathbf{L} \to \mathbf{K}$ define a congruence $\equiv$ on $\mathbf{L}$ whose quotient $\mathbf{L}/{\equiv}$ is isomorphic to $\mathbf{K}$.

3.2. **The excedance relation on permutations.** We now recall the amazing properties of the excedance relation on permutations defined in [BG24].

A *noncrossing partition* (NCP) of $[n]$ is a collection $\lambda \subseteq \{(i,j) \mid 1 \le i \le j \le n\}$ such that there is no $(i,j),(k,\ell) \in \lambda$ with $i \le k < j \le \ell$. Equivalently, it is a collection of arcs over the points $1,\dots,n$ on the horizontal line, such that any two arcs do not cross in their interior, nor share their left endpoints nor their right endpoints. We denote by $\lambda^- := \{i \mid (i,j) \in \lambda\}$ the set of left endpoints and $\lambda^+ := \{j \mid (i,j) \in \lambda\}$ the set of of right endpoints of λ. We denote by $\mathbf{NCP}_n$ the transitive closure of the relation $\prec$ on NCPs of $[n]$ defined by $\lambda \prec \mu$ if and only if $\lambda = \mu \smallsetminus \{(i,i+1)\}$ for some $i \in [n-1]$ or $\lambda = \mu \smallsetminus \{(i,k)\} \cup \{(i,j),(j,k)\}$ for some $1 \le i < j < k \le n$. Note that the standard bijection between Dyck paths of semilength n and NCPs of $[n]$ (see Figure 9) sends the Stanley lattice $\mathbf{Dyck}_n$ to the lattice $\mathbf{NCP}_n$ (see Figure 10).

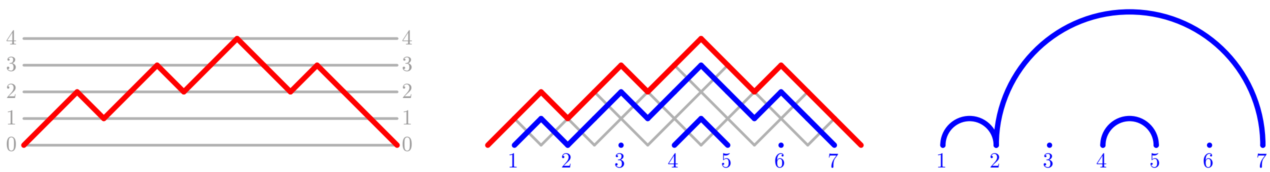

FIGURE 9. The standard bijection from Dyck paths (left) to NCPs (right).

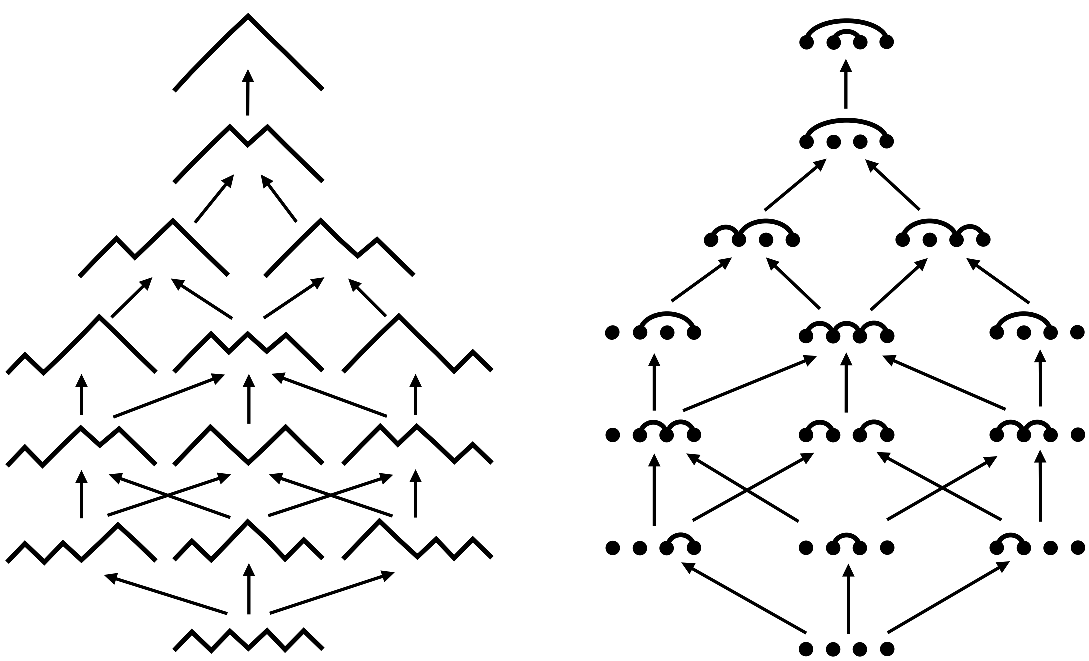

FIGURE 10. The Stanley lattice $\mathbf{Dyck}_4$ on Dyck paths of semilength 4 (left) is isomorphic to the lattice $\mathbf{NCP}_n$ on noncrossing partitions of [4] (right).

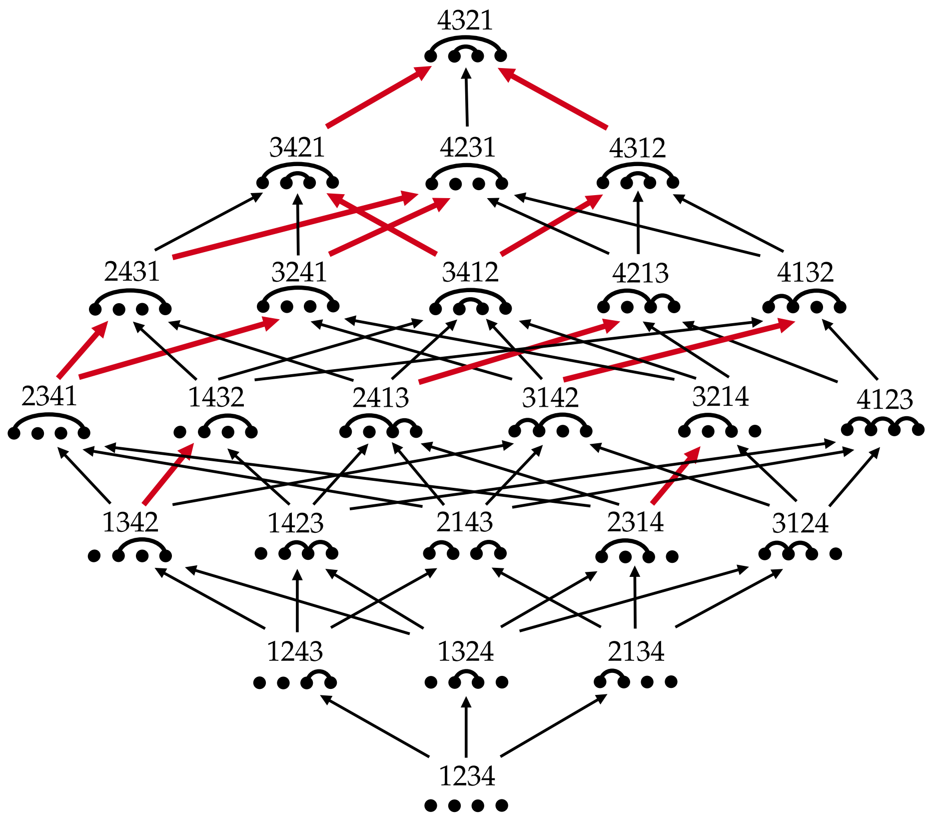

FIGURE 11. The excedance relation on the Bruhat order on $\mathfrak{S}_4$. Cover relations between two excedance equivalent permutations are red and bolded.

Definition 3.1 ([BG24]). *A weak excedance of a permutation $\sigma \in \mathfrak{S}_n$ is a pair (i, σ_i) such that $i \leq \sigma_i$. Define the excedance positions $\mathrm{E}_{\mathrm{pos}}(\sigma) := \{i \mid i \leq \sigma_i\}$ and the excedance values $\mathrm{E}_{\mathrm{val}}(\sigma) := \{\sigma_i \mid i \leq \sigma_i\}$. The excedance relation on $\mathfrak{S}_n$ is defined by $\sigma \equiv \tau$ if and only if $\mathrm{E}_{\mathrm{pos}}(\sigma) = \mathrm{E}_{\mathrm{pos}}(\tau)$ and $\mathrm{E}_{\mathrm{val}}(\sigma) = \mathrm{E}_{\mathrm{val}}(\tau)$. We denote by $\mathfrak{S}_n/\!\equiv$ the poset quotient on equivalence classes of $\equiv$, defined by $X \leq Y$ if and only if there are representatives $x \in X$ and $y \in Y$ such that $x \leq y$ in Bruhat order. See Figure 11 for an illustration when $n = 4$.*

Definition 3.2 ([BG24]). *For $\lambda \in \mathbf{NCP}_n$, define two permutations σ_λ and τ_λ of $[n]$ by*

$$\sigma_\lambda(j) := \begin{cases} r\text{-th element of } \lambda^+ & \text{if } i \text{ is the } r\text{-th element of } \lambda^- \\ r\text{-th element of } [n] \smallsetminus \lambda^+ & \text{if } i \text{ is the } r\text{-th element of } [n] \smallsetminus \lambda^- \end{cases}$$

and

$$\tau_\lambda(j) := \begin{cases} i & \text{if } j \notin \lambda^- \text{ and } (i,j) \in \lambda \\ \text{maximum of the connected component of } j \text{ in } \lambda & \text{if } j \notin \lambda^- \end{cases}$$

and the set of permutations

$$C_\lambda := \left\{\sigma \in \mathfrak{S}_n \;\middle|\; \mathrm{E}_{\mathrm{pos}}(\sigma) = [n] \smallsetminus \lambda^- \text{ and } \mathrm{E}_{\mathrm{val}}(\sigma) = [n] \smallsetminus \lambda^+\right\}.$$

Note that the permutations τ_λ where already considered by M. Zinno [Zin02] and known to provide a basis of the Temperley–Lieb algebra (see Section 7 for details). N. Bergeron and L. Gagnon extended this as follows [BG24].

Theorem 3.3 ([BG24])**.** *For any $n \in \mathbb{N}$,*

(1) For any $\lambda \in \mathbf{NCP}_n$, the permutation σ_λ (resp. τ_σ) avoids the pattern 321 (resp. 3412).
(2) For any $\lambda \in \mathbf{NCP}_n$, the set C_λ is the interval $[\sigma_\lambda, \tau_\lambda]$ of the Bruhat order on $\mathfrak{S}_n$.
(3) The map $\lambda \mapsto C_\lambda$ is a bijection from the NCPs of $[n]$ to the excedance classes of $\mathfrak{S}_n$.
(4) The quotient $\mathfrak{S}_n/\equiv$ is isomorphic to the Stanley lattice: $\lambda \le \mu$ if and only if $C_\lambda \le C_\mu$.
(5) Any choice of representatives of the excedance classes yields a basis of the Temperley–Lieb algebra $\mathrm{TL}_n(2)$ (see Section 7 for details).

3.3. **The excedance congruence on ASM.** We now extend the excedance relation on permutations to a lattice congruence on $\mathbf{ASM}_n$. For this, we consider the diagonal and the superdiagonal of the corresponding HFMs.

Definition 3.4. *The excedance congruence of $\mathbf{HFM}_n$ is the equivalence relation $\equiv$ defined by $H \equiv H'$ if and only if $H_{i,j} = H'_{i,j}$ for all $0 \le i, j \le n$ with $j - i \in \{0, 1\}$. The excedance congruence of $\mathbf{ASM}_n$ is the corresponding equivalence relation $\equiv$ on $\mathbf{ASM}_n$.*

Lemma 3.5. *The excedance congruence is a lattice congruence on $\mathbf{HFM}_n$ (or $\mathbf{ASM}_n$).*

Proof. Let $H \equiv H'$ and $K \equiv K'$ in $\mathbf{HFM}_n$. For any $0 \le i, j \le n$ with $j - i \in \{0, 1\}$, we have $H_{i,j} = H'_{i,j}$ and $K_{i,j} = K'_{i,j}$, hence $(H \vee K)_{i,j} = \max(H_{i,j}, K_{i,j}) = \max(H'_{i,j}, K'_{i,j}) = (H' \vee K')_{i,j}$. We conclude that $H \vee K \equiv H' \vee K'$. The proof is symmetric for the meet. □

We now check that the excedance relation on alternating sign matrices restricts to the excedance relation on permutations. Denote by P_σ the permutation matrix of $\sigma \in \mathfrak{S}_n$, that is, where $(P_\sigma)_{i,j} = \delta_{\sigma_i, j}$ for all $i, j \in [n]$.

Lemma 3.6. *For any permutations $\sigma, \tau \in \mathfrak{S}_n$, we have $\sigma \equiv \tau$ if and only if $P_\sigma \equiv P_\tau$.*

Proof. Note that for an ASM A with HFM H, we have $H_{i,i} - H_{i,i+1} = 2\sum_{i'<i} A_{i',i} - 1$. For $A = P_\sigma$, we thus obtain that $H_{i,i} - H_{i,i+1} = 1$ if and only if $i \in \mathrm{E}_{\mathrm{val}}(\sigma)$. Similarly, $H_{i,i+1} - H_{i+1,i+1} = 1$ if and only if $i \in \mathrm{E}_{\mathrm{pos}}(\sigma)$. Finally, recall that $H_{i,i} - H_{i,i+1} \in \{-1, 1\}$ and $H_{i,i+1} - H_{i+1,i+1} \in \{-1, 1\}$. Consequently, the values $H_{i,j}$ for $i, j \in [n]$ with $j - i \in \{0, 1\}$ and the pair $\big(\mathrm{E}_{\mathrm{pos}}(\sigma), \mathrm{E}_{\mathrm{val}}(\sigma)\big)$ determine each other. □

We will now describe the classes of the excedance congruence. For this, define the *height sequence* of a Dyck path as the sequence of heights of its integer points (see Figure 12).

Lemma 3.7. *For any HFM H, the sequence $H_{1,1}, H_{1,2}, H_{2,2}, H_{2,3}, \dots, H_{n-1,n-1}, H_{n-1,n}, H_{n,n}$ is the height sequence of a Dyck path.*

Proof. It immediately follows from the fact that $H_{1,1} = 0 = H_{n,n}$ and that $H_{i,j} \ge 0$ and $H_{i,j} - H_{i,j+1} \in \{-1, 1\}$ and $H_{i,j} - H_{i+1,j} \in \{-1, 1\}$ for any $i, j \in [n]$. □

Combining Lemma 3.7 with the bijections between ASMs and HFMs and between NCPs, Dyck paths, and height sequences, we obtain a map $A \mapsto \boldsymbol{\lambda}(A)$ from ASMs to NCPs. See Figure 12 for an illustration.

$$\begin{pmatrix} \cdot & + & \cdot & \cdot & \cdot & \cdot & \cdot \\ \cdot & \cdot & \cdot & \cdot & \cdot & + & \cdot \\ \cdot & \cdot & + & \cdot & \cdot & - & + \\ \cdot & \cdot & \cdot & \cdot & + & \cdot & \cdot \\ + & \cdot & - & + & \cdot & \cdot & \cdot \\ \cdot & \cdot & \cdot & \cdot & \cdot & + & \cdot \\ \cdot & \cdot & + & \cdot & \cdot & \cdot & \cdot \end{pmatrix} \qquad \begin{pmatrix} \mathbf{0} & \mathbf{1} & 2 & 3 & 4 & 5 & 6 & 7 \\ 1 & \mathbf{2} & \mathbf{1} & 2 & 3 & 4 & 5 & 6 \\ 2 & 3 & \mathbf{2} & \mathbf{3} & 4 & 5 & 4 & 5 \\ 3 & 4 & 3 & \mathbf{2} & \mathbf{3} & 4 & 5 & 4 \\ 4 & 5 & 4 & 3 & \mathbf{4} & \mathbf{3} & 4 & 3 \\ 5 & 4 & 3 & 4 & 3 & \mathbf{2} & \mathbf{3} & 2 \\ 6 & 5 & 4 & 5 & 4 & 3 & \mathbf{2} & \mathbf{1} \\ 7 & 6 & 5 & 4 & 3 & 2 & 1 & \mathbf{0} \end{pmatrix}$$

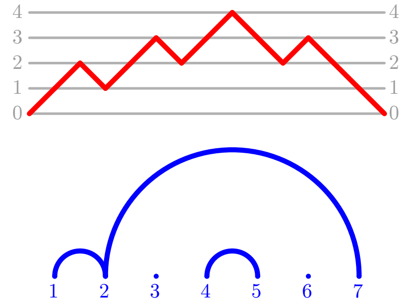

FIGURE 12. An ASM (left), its HFM (middle), its Dyck path (top right), and its NCP (bottom right).

Definition 3.8. *For $\lambda \in \mathbf{NCP}_n$, we define the set of ASMs*

$$D_\lambda := \{A \in \mathbf{ASM}_n \mid \boldsymbol{\lambda}(A) = \lambda\}.$$

Lemma 3.9. *For any $\lambda \in \mathbf{NCP}_n$, we have $C_\lambda = \{\sigma \in \mathfrak{S}_n \mid P_\sigma \in D_\lambda\}$.*

Proof. Same arguments as in Lemma 3.6. □

Lemma 3.10. *The map $\lambda \mapsto D_\lambda$ is a bijection from the NCPs of $[n]$ to the excedance classes of $\mathbf{ASM}_n$.*

Proof. For $A, A' \in \mathbf{ASM}_n$ with corresponding $H, H' \in \mathbf{HFM}_n$, we have $\boldsymbol{\lambda}(A) = \boldsymbol{\lambda}(A')$ if and only if H and H' have the same diagonal and superdiagonal, that is $H \equiv H'$, that is $A \equiv A'$. □

Lemma 3.11. *For any NCP λ, the maximal ASM of the class D_λ is the permutation matrix P_{τ_λ}.*

Proof. We skip the proof that the maxima of classes are always permutation matrices as it will be proved in more generality in Section 5. The result then follows from Lemma 3.9 and Theorem 3.3 (2). □

In contrast, note that the minima of excedance classes on $\mathbf{ASM}_n$ are not permutation matrices in general, although it follows from Lemma 3.9 and Theorem 3.3 (2) that each excedance class D_λ contains a minimal permutation matrix P_{σ_λ}.

Corollary 3.12. *The lattice quotient $\mathbf{ASM}_n/\!\equiv$ is isomorphic to the Stanley lattice: $\lambda \leq \mu$ if and only if $D_\lambda \leq D_\mu$.*

Proof. This follows from Lemma 3.11 and Theorem 3.3 (4). □

The goal of this paper is to show that all properties of Theorem 3.3 actually hold for any lattice quotient of $\mathbf{ASM}_n$ isomorphic to $\mathbf{Dyck}_n$.

4. Catalan congruences of $\mathbf{ASM}_n$

This paper focuses on the following generalization of Section 3.3.

Definition 4.1. *A catalan congruence is a congruence of the lattice $\mathbf{ASM}_n$ on alternating sign matrices whose quotient is isomorphic to the Stanley lattice $\mathbf{Dyck}_n$ on Dyck paths.*

The two catalan congruences when $n = 3$ are represented in Figure 13. In this section, we describe all catalan congruences and encode them bijectively using several combinatorial structures, namely walls, depth triangles, catalan triangles and bicolored pipe dreams.

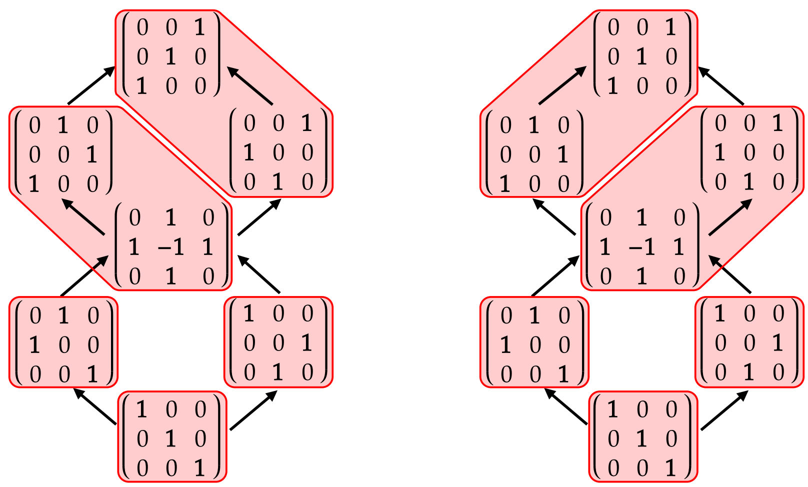

Figure 13. The two lattice congruences $\mathbf{ASM}_3$ whose quotient are isomorphic to $\mathbf{Dyck}_3$.

4.1. Quotients of distributive lattices.

Quotients of distributive lattices are distributive (by the definition of $\vee$ and $\wedge$ on $\mathbf{L}/\!\equiv$), and behave properly with respect to Birkhoff's fundamental theorem of distributive lattices (Theorem 2.1). Recall that we denote by $j_\star$ the single element covered by a join irreducible j.

Theorem 4.2. *For a congruence $\equiv$ on a distributive lattice $\mathbf{L}$, denote by $\mathcal{J}(\equiv)$ the subposet of $\mathcal{J}(\mathbf{L})$ induced by the join irreducibles j such that $j \not\equiv j_\star$. Then*

- *an element $x \in \mathbf{L}$ is minimal in its congruence class if and only if the corresponding antichain $\mathrm{j}(x)$ is contained in $\mathcal{J}(\equiv)$,*
- *the quotient $\mathbf{L}/\!\equiv$ is isomorphic to the distributive lattice of lower sets of $\mathcal{J}(\equiv)$.*

Dual statements hold for meet irreducibles.

This yields in particular the following statement.

Theorem 4.3 ([Thu54])**.** *Given two finite distributive lattices $\mathbf{L}$ and $\mathbf{K}$, the lattice congruences of $\mathbf{L}$ whose quotients are isomorphic to $\mathbf{K}$ are in bijection with the subposets of $\mathcal{J}(\mathbf{L})$ isomorphic to $\mathcal{J}(\mathbf{K})$.*

4.2. **Walls.** We now specialize Theorem 4.3 to understand all catalan congruences. We have seen in Section 2 that $\mathcal{J}(\mathbf{ASM}_n)$ is isomorphic to the tetrahedron poset $\mathcal{T}_n$, and $\mathcal{J}(\mathbf{Dyck}_n)$ is isomorphic to the triangular poset $\mathcal{D}_n$ (see Figure 3). Hence, by Theorem 4.3, quotients of $\mathbf{ASM}_n$ isomorphic to $\mathbf{Dyck}_n$ are in bijection with subposets of $\mathcal{T}_n$ isomorphic to $\mathcal{D}_n$. We now show that this isomorphism always factorizes through the horizontal projection $(x_1, x_2, x_3, x_4) \mapsto (x_1, x_2 + x_3, x_4)$ of $\mathcal{T}_n$.

Proposition 4.4. *Let $\mathcal{P}$ be a subposet of the tetrahedron poset $\mathcal{T}_n$ isomorphic to the triangular poset $\mathcal{D}_n$. For any $(y_1, y_2, y_3) \in \mathcal{D}_n$, the subposet $\mathcal{P}$ contains exactly one element (x_1, x_2, x_3, x_4) such that $x_1 = y_1$ and $x_4 = y_3$ (and thus $x_2 + x_3 = y_2$).*

Proof. The posets $\mathcal{T}_n$ and $\mathcal{D}_n$ are both ranked of height $n-2$ and therefore any morphism must preserve the rank. Namely, $\mathcal{T}_n$ has rank function $(x_1, x_2, x_3, x_4) \mapsto x_2 + x_3$ and $\mathcal{D}_n$ has rank function $(y_1, y_2, y_3) \mapsto y_2$. Hence, any subposet $\mathcal{P} \subset \mathcal{T}_n$ isomorphic to $\mathcal{D}_n$ must contain $n-1-i$ elements of rank i for all $0 \le i \le n-2$. Therefore, $\mathcal{P}$ cannot contain two distinct elements $\mathbf{x}$ and $\mathbf{w}$ where $x_1 = w_1$ and $x_4 = w_4$, since there would be $x_2 + x_3 + 1$ elements of rank 0 lesser than $\mathbf{x}$ or $\mathbf{w}$ in $\mathcal{T}_n$, but two distinct elements of rank $x_2 + x_3$ in $\mathcal{D}_n$ should have at least $x_2 + x_3 + 2$ elements of rank 0 lesser than them. ☐

In other words, Proposition 4.4 states that the subposets of $\mathcal{T}_n$ isomorphic to $\mathcal{D}_n$ can be seen as vertical (possibly undulating) sections of $\mathcal{T}_n$, which motivates the following name.

Definition 4.5. *A wall of order n is a subposet of $\mathcal{T}_n$ isomorphic to $\mathcal{D}_n$.*

Example 4.6. *The excedance quotient of Section 3.3 is given by the undulating wall*

$$\{(x_1, x_2, x_3, x_4) \in \mathcal{T}_n \mid x_3 - x_2 \in \{0, -1\}\}.$$

See Figure 18 (left).

We will also need the following observation. Visually, it states that a wall cannot enter the interior of the black butterfly illustrated in Figure 27 (left) at each of its points.

Lemma 4.7. *If (x_1, x_2, x_3, x_4) and (x'_1, x'_2, x'_3, x'_4) are in a wall, then $x'_2 - x_2$, $x_3 - x'_3$, $x'_1 + x'_2 - x_1 - x_2$ and $x_1 + x_3 - x'_1 - x'_3$ cannot be all strictly positive or all strictly negative.*

Proof. Consider $\boldsymbol{x} := (x_1, x_2, x_3, x_4)$ and $\boldsymbol{x}' := (x'_1, x'_2, x'_3, x'_4)$ in a wall, and the corresponding projections $\boldsymbol{y} := (x_1, x_2 + x_3, x_4)$ and $\boldsymbol{y}' := (x'_1, x'_2 + x'_3, x'_4)$. There is a (non-directed) path of cover relations of $\mathcal{D}_n$ joining $\boldsymbol{y}$ to $\boldsymbol{y}'$. Lifting this path to the wall, we obtain a path from $\boldsymbol{x}$ to $\boldsymbol{x}'$ which avoids the interior of the butterfly at $\boldsymbol{x}$. ☐

4.3. **Depth triangles.** For any wall $\mathcal{P} \subset \mathcal{T}_n$, Proposition 4.4 ensures that the horizontal projection $(x_1, x_2, x_3, x_4) \mapsto (x_1, x_2 + x_3, x_4)$ is a bijection from $\mathcal{P}$ to $\mathcal{D}_n$. We can therefore encode the wall $\mathcal{P}$ by recording the depth $x_3 - x_2$ of the point (x_1, x_2, x_3, x_4) in the direction of the projection. See Figure 15. We now characterize the triangular arrays obtained this way.

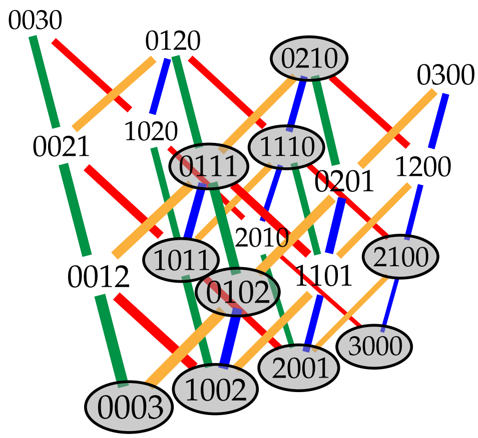

$$\begin{array}{ccccccc} & & & -1 & & & \\ & & 0 & & 0 & & \\ & -1 & & 1 & & -1 & \\ 0 & & 0 & & 0 & & 0 \end{array} \qquad \begin{array}{ccccccc} & & & 2 & & & \\ & & 2 & & 3 & & \\ & 1 & & 3 & & 3 & \\ 1 & & 2 & & 3 & & 4 \end{array}$$

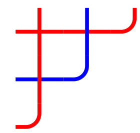

FIGURE 15. A subposet of $\mathcal{T}_5$ isomorphic to $\mathcal{D}_5$ (left) and its corresponding depth triangle (middle left), catalan triangle (middle right), and bicolored pipe dream (right).

Definition 4.8. *A depth triangle of order n is a map $\delta : \mathcal{D}_n \to \mathbb{Z}$ such that*

- *the bottom row is $00\cdots0$, that is, $\delta(i, 0, n-2-i) = 0$ for all $0 \le i \le n-2$,*
- $|\delta(y_1, y_2, y_3) - \delta(y_1, y_2 - 1, y_3 + 1)| = 1 = |\delta(y_1, y_2, y_3) - \delta(y_1 + 1, y_2 - 1, y_3)|$.

Note that a depth triangle of order n has $n-1$ rows (or diagonals). See Figure 14.

$$\begin{array}{ccccc} & & -2 & & \\ & -1 & & -1 & \\ 0 & & 0 & & 0 \end{array} \quad \begin{array}{ccccc} & & 0 & & \\ & -1 & & -1 & \\ 0 & & 0 & & 0 \end{array} \quad \begin{array}{ccccc} & & 0 & & \\ & 1 & & -1 & \\ 0 & & 0 & & 0 \end{array} \quad \begin{array}{ccccc} & & 0 & & \\ & -1 & & 1 & \\ 0 & & 0 & & 0 \end{array} \quad \begin{array}{ccccc} & & 0 & & \\ & 1 & & 1 & \\ 0 & & 0 & & 0 \end{array} \quad \begin{array}{ccccc} & & 2 & & \\ & 1 & & 1 & \\ 0 & & 0 & & 0 \end{array}$$

FIGURE 14. The 6 depth triangles of order 4.

Example 4.9. *Following Example 4.6, the depth triangle of the excedance quotient of Section 3.3 is given by $\delta(y_1, y_2, y_3) = 2\lfloor y_2/2 \rfloor - y_2 = -(y_2 \mod 2)$ (in other words, odd rows are 0 while even rows are -1). See Figure 18 (middle left).*

Theorem 4.10. *The catalan congruences of $\mathbf{ASM}_n$ are in bijection with the depth triangles of order n.*

Proof. We have shown in Proposition 4.4 that subposets $\mathcal{P} \subset \mathcal{T}_n$ isomorphic to $\mathcal{D}_n$ can be encoded by triangles of numbers. Namely, if $(y_1, y_2, y_3) \in \mathcal{D}_n$ and (x_1, x_2, x_3, x_4) is the only element of $\mathcal{P}$ such that $x_1 = y_1$ and $x_4 = y_3$, then we define the depth $\delta(y_1, y_2, y_3) = x_3 - x_2$. See Figure 15 for an illustration. These triangles are clearly exactly the depth triangles. $\square$

Proposition 4.11. *For any depth triangle δ, we have*

- $-y_2 \le \delta(y_1, y_2, y_3) \le y_2$ *and* $\delta(y_1, y_2, y_3) \equiv_{\text{mod } 2} y_2$ *for all* $(y_1, y_2, y_3) \in \mathcal{D}_n$, *and*
- $|\delta(z_1, z_2, z_3) - \delta(y_1, y_2, y_3)| \le |y_1 - z_1| + |y_3 - z_3|$ *for all* $(y_1, y_2, y_3), (z_1, z_2, z_3) \in \mathcal{D}_n$.

Proof. Immediately follows from the two conditions of Definition 4.8. $\square$

4.4. **Catalan triangles.** By an appropriate shift of the entries, we now connect the depths triangles of Section 4.3 to certain Gelfand–Tsetlin patterns. A *Gelfand–Tsetlin pattern* of order n is a map $\gamma : \mathcal{D}_n \to \mathbb{N}$ subject to the interlacing conditions

$$\gamma(y_1, y_2 - 1, y_3 + 1) \leq \gamma(y_1, y_2, y_3) \leq \gamma(y_1 + 1, y_2 - 1, y_3).$$

Again, note that a Gelfand–Tsetlin pattern of order n has $n - 1$ rows (or diagonals). We say that γ is *doubly gapless* if moreover

$$\gamma(y_1, y_2, y_3) - \gamma(y_1, y_2 - 1, y_3 + 1) \leq 1 \quad \text{and} \quad \gamma(y_1 + 1, y_2 - 1, y_3) - \gamma(y_1, y_2, y_3) \leq 1.$$

We note that our definition of Gelfand–Tsetlin patterns only differs from the classical definition by our use of barycentric coordinates to parametrize $\mathcal{D}_n$. We also observe that our two conditions for doubly gapless patterns are usually called gapless and left-gapless. Gapless triangles were introduced by A. Ayyer, R. Cori and D. Gouyou-Beauchamps [ACGB11], who described a bijection between gapless Gog triangles and gapless Magog triangles.

Definition 4.12. *A catalan triangle of order n is a doubly gapless Gelfand–Tsetlin pattern with bottom row $12 \cdots (n-1)$. See Figure 16.*

1	2	2	2	2	3
1 2	1 2	2 2	1 3	2 3	2 3
1 2 3	1 2 3	1 2 3	1 2 3	1 2 3	1 2 3

FIGURE 16. The 6 catalan triangles of order 4.

Example 4.13. *Following Examples 4.6 and 4.9, the catalan triangle of the excedance quotient of Section 3.3 is given by $\gamma(y_1, y_2, y_3) = y_1 + \lfloor y_2/2 \rfloor + 1$. See Figure 18 (middle right).*

Proposition 4.14. *The depth triangles of order n are in bijection with the catalan triangles of order n.*

Proof. The bijection is given by the formula $\gamma(y_1, y_2, y_3) = \delta(y_1, y_2, y_3)/2 + y_1 + y_2/2 + 1$. See Figure 19. □

Proposition 4.15. *For any catalan triangle γ, we have*

- $y_1 + 1 \leq \gamma(y_1, y_2, y_3) \leq y_1 + y_2 + 1 = n - 1 - y_3$ *for all* $(y_1, y_2, y_3) \in \mathcal{D}_n$, *and*
- $0 \leq \gamma(z_1, z_2, z_3) - \gamma(y_1, y_2, y_3) \leq z_1 - y_1 + y_3 - z_3$ *for all* $(y_1, y_2, y_3), (z_1, z_2, z_3) \in \mathcal{D}_n$ *with* $y_1 \leq z_1$ *and* $y_3 \geq z_3$.

Proof. Immediately follows from the two conditions of Definition 4.8, or from the combination of Propositions 4.11 and 4.14. □

4.5. **Bicolored pipe dreams.** We now connect depth triangles and catalan triangles to certain pipe dreams. A *pipe dream* P is a filling of a triangular shape with crossings $+$ and contacts so that all pipes entering on the left side exit on the top side [BB93, KM05]. The *contact graph* of P is the graph with a vertex for each pipe of P and an edge between two pipes if they share a contact. We say that P is *connected* (resp. bipartite) if its contact graph is.

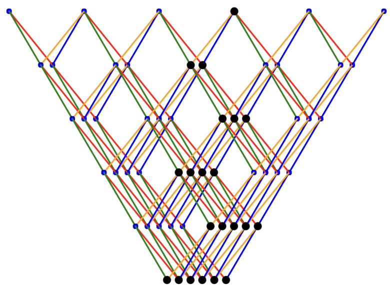

$$\begin{array}{ccccccccccc} & & & & & -1 & & & & & \\ & & & & 0 & & 0 & & & & \\ & & & -1 & & -1 & & -1 & & & \\ & & 0 & & 0 & & 0 & & 0 & & \\ & -1 & & -1 & & -1 & & -1 & & -1 & \\ 0 & & 0 & & 0 & & 0 & & 0 & & 0 \end{array} \qquad \begin{array}{ccccccccccc} & & & & & 3 & & & & & \\ & & & & 3 & & 4 & & & & \\ & & & 2 & & 3 & & 4 & & & \\ & & 2 & & 3 & & 4 & & 5 & & \\ & 1 & & 2 & & 3 & & 4 & & 5 & \\ 1 & & 2 & & 3 & & 4 & & 5 & & 6 \end{array}$$

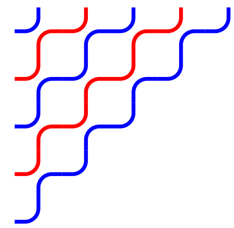

FIGURE 18. The wall (left), depth triangle (middle left), catalan triangle (middle right), and bicolored pipe dream (right) corresponding to the excedance quotient of [BG24].

Definition 4.16. *A bicolored pipe dream is a pipe dream whose pipes are colored red or blue so that each contact is bichromatic. In other words, it is a pipe dream together with a proper bicoloration of its contact graph. Note that there is no color restriction on the crossings: they are allowed to be both monocolor or bicolor. See Figure 17.*

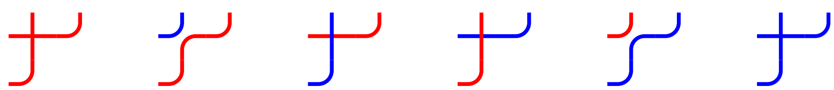

FIGURE 17. The 6 bicolored pipe dreams with 2 pipes.

Example 4.17. *Following Examples 4.6, 4.9 and 4.13, the bicolored pipe dream of the excedance quotient of Section 3.3 is the pipe dream with no crossing (hence waving pipes alternating colors), whose longest pipe is blue. See Figure 18 (right).*

Proposition 4.18. *The depth triangles (or equivalently the catalan triangles) of order n are in bijection with the bicolored pipe dreams with $n-2$ pipes.*

Proof. In a depth triangle, we draw a red (resp. blue) line between two adjacent entries such that $\delta(y_1, y_2, y_3) > \delta(y_1, y_2-1, y_3+1)$ or $\delta(y_1, y_2, y_3) < \delta(y_1+1, y_2-1, y_3)$ (resp. $\delta(y_1, y_2, y_3) < \delta(y_1, y_2-1, y_3+1)$ or $\delta(y_1, y_2, y_3) > \delta(y_1+1, y_2-1, y_3)$). In a catalan triangle, we draw a red (resp. blue) line between two adjacent entries such that $\delta(y_1, y_2, y_3) = \delta(y_1, y_2-1, y_3+1)$ or $\delta(y_1, y_2, y_3) < \delta(y_1+1, y_2-1, y_3)$ (resp. $\delta(y_1, y_2, y_3) < \delta(y_1, y_2-1, y_3+1)$ or $\delta(y_1, y_2, y_3) = \delta(y_1+1, y_2-1, y_3)$). See Figure 19. $\square$

By definition, a bicolored pipe dream is bipartite, but a bipartite pipe dream admits several bicolorations. Namely, one can switch the two colors on any connected component of the contact graph and preserve a proper bicoloration. This immediately yields the following statement connecting the numbers of Table 1.

Proposition 4.19. *Denote by*

$$\mathrm{CT} := \sum_{n\geq 0} \mathrm{CT}_n \frac{x^n}{n!}, \quad \mathrm{BPD} := \sum_{n\geq 0} \mathrm{BPD}_n \frac{x^n}{n!} \quad \textit{and} \quad \mathrm{BCPD} := \sum_{n\geq 0} \mathrm{BCPD}_n \frac{x^n}{n!}$$

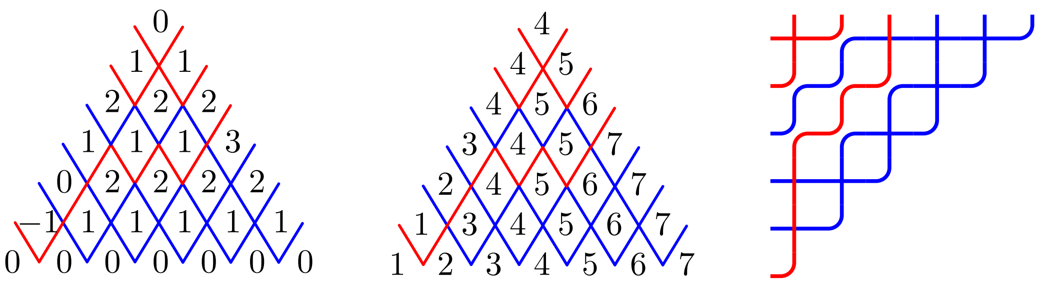

FIGURE 19. Bijection between depth triangles (left), catalan triangles (middle) and bicolored pipe dreams (right).

n	0	1	2	3	4	5	6	7	$\cdots$
CT_n	1	2	6	28	202	2252	38756	1028964	$\cdots$
BPD_n	1	1	2	8	57	681	12942	379326	$\cdots$
BCPD_n	0	1	1	4	31	420	8936	287702	$\cdots$

TABLE 1. Number of catalan triangles, bipartite pipe dreams and bipartite connected pipe dreams.

the exponential generating functions of the numbers of catalan triangles of order n, and of the numbers of bipartite (resp. bipartite connected) pipe dreams with $n-2$ pipes. Then

$$\mathrm{CT} = \exp\bigl(2\,\mathrm{BCPD}\bigr) = \mathrm{BPD}^2\,.$$

Proof. Since a bipartite pipe dream is a shuffle of connected bipartite pipe dreams, we have $\exp\bigl(\mathrm{BCPD}\bigr) = \mathrm{BPD}$. Since each connected component of a bipartite pipe dream can be colored two ways, we have $\mathrm{CT} = \exp\bigl(2\,\mathrm{BCPD}\bigr)$. The result follows. $\square$

We also obtain the following formula, similar to the 2-enumeration of ASMs.

Proposition 4.20. *We have $\sum_P 2^{\mathrm{bcc}(P)} = 2^{\binom{n}{2}}$, where the sum ranges over the bicolored pipe dreams P with n pipes, and $\mathrm{bcc}(P)$ denotes the number of bicolored crossings of P.*

Proof. Given a triangle of $\binom{n}{2}$ Boolean variables, we construct a bicolored pipe dream as follows (see Figure 20). We start from the diagonal and take the Boolean values along the diagonal as the colors of the elbows. Then we move upward in the northwest direction, applying the following rule at each intersection:

- If the two strands arriving from the south and the east have the same color, then we use the Boolean value at this intersection to choose between placing a crossing or a contact, and we color the strands leaving to the north and the west accordingly (same color as the arriving strands if we choose a crossing, distinct color from the arriving strands if we choose a contact).
- If the two strands arriving from the south and the east have different colors, then we ignore the Boolean value at this intersection as we must place a crossing, and each strand keeps its color.

T	F	?	T	T	T
F	F	F	T	T	
F	F	T	T		
?	T	T			
?	T				
F					

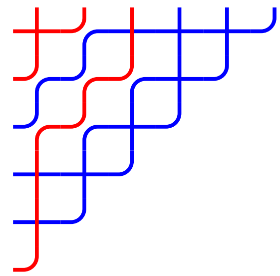

FIGURE 20. The map between Boolean triangles (left) and bicolored pipe dreams (right) described in the proof of Proposition 4.20. The question marks can be replaced by any Boolean values, since they are ignored during the procedure as the two strands arriving from the south and the east have different colors.

This procedure clearly constructs a bicolored pipe dream, and every such bicolored pipe dream P arises with multiplicity $2^{\mathrm{bcc}(P)}$, since each bicolored crossing of P corresponds to an ignored Boolean value during this procedure. $\square$

4.6. **The lattice of catalan triangles.** Finally, we note that the set of catalan triangles carries itself a natural distributive lattice structure, whose join irreducible poset is illustrated in Figure 23.

Proposition 4.21. *The set of catalan triangles of order n ordered by coordinatewise comparison forms a distributive lattice $\mathbf{Cat}_n$, whose join-irreducibles poset is isomorphic to the poset of quadruples $(x_1, x_2, x_3, x_4) \in \mathbb{N}^4$ with $x_1 + x_2 + x_3 + x_4 = n - 2$, ordered by $\mathbf{x} \le \mathbf{y}$ if and only if $x_2 + x_3 + x_4 \le y_2 + y_3 + y_4$, $x_2 + x_4 \le y_2 + y_4$, $x_3 + x_4 \le y_3 + y_4$ and $x_4 \le y_4$.*

Proof. The set of catalan triangles of order n is closed under coordinatewise maximum and minimum, making it a distributive lattice. Each join irreducible catalan triangle corresponds to one entry of the depth triangle with non-minimal depth, which corresponds to elements of $\mathcal{T}_n$ not in the minimal wall. More precisely, to each quadruple (x_1, x_2, x_3, x_4) with $x_1 + x_2 + x_3 + x_4 = n - 2$ corresponds the smallest catalan triangle with $\gamma(x_3, x_1 + x_4 + 1, x_2) = x_3 + x_4 + 2$. The order on join-irreducible catalan triangles is obtained by reorienting edges in $\mathcal{T}_n$ horizontally. $\square$

Remark 4.22. *By Propositions 4.14 and 4.18, Proposition 4.21 also translates to the depth triangles of Section 4.3 and the bicolored pipe dreams of Section 4.5.*

Example 4.23. *The minimum (resp. maximum) depth triangles, catalan triangles, and bicolored pipe dreams are given by:*

- $\delta_{\min}(y_1, y_2, y_3) = -y_2$ *(resp.* $\delta_{\max}(y_1, y_2, y_3) = y_2$*),*
- $\gamma_{\min}(y_1, y_2, y_3) = y_1 + 1$ *(resp.* $\gamma_{\max}(y_1, y_2, y_3) = y_1 + y_2 + 1 = n - 1 - y_3$*),*
- *the completely red (resp. blue) pipe dreams with only crossings.*

See Figures 21 and 22.

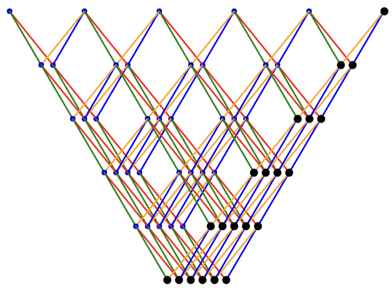

$$\begin{array}{cccccc} & & -5 & & & \\ & & -4 & -4 & & \\ & -3 & -3 & -3 & & \\ & -2 & -2 & -2 & -2 & \\ -1 & -1 & -1 & -1 & -1 & \\ 0 & 0 & 0 & 0 & 0 & 0 \end{array} \qquad \begin{array}{c} 1 \\ 1\ \ 2 \\ 1\ \ 2\ \ 3 \\ 1\ \ 2\ \ 3\ \ 4 \\ 1\ \ 2\ \ 3\ \ 4\ \ 5 \\ 1\ \ 2\ \ 3\ \ 4\ \ 5\ \ 6 \end{array}$$

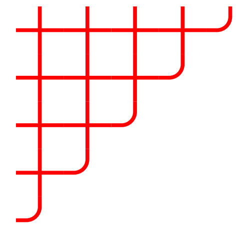

FIGURE 21. The minimal wall (left), depth triangle (middle left), catalan triangle (middle right), and bicolored pipe dream (right).

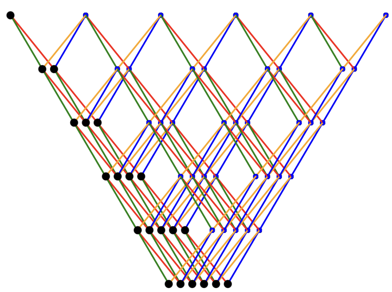

$$\begin{array}{c} 5 \\ 4\ \ 4 \\ 3\ \ 3\ \ 3 \\ 2\ \ 2\ \ 2\ \ 2 \\ 1\ \ 1\ \ 1\ \ 1\ \ 1 \\ 0\ \ 0\ \ 0\ \ 0\ \ 0\ \ 0 \end{array} \qquad \begin{array}{c} 6 \\ 5\ \ 6 \\ 4\ \ 5\ \ 6 \\ 3\ \ 4\ \ 5\ \ 6 \\ 2\ \ 3\ \ 4\ \ 5\ \ 6 \\ 1\ \ 2\ \ 3\ \ 4\ \ 5\ \ 6 \end{array}$$

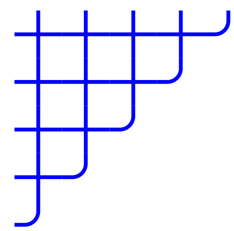

FIGURE 22. The maximal wall (left), depth triangle (middle left), catalan triangle (middle right), and bicolored pipe dream (right).

4.7. **Symmetric and self-dual catalan triangles.** The lattice $\mathbf{Cat}_n$ has an automorphism given by $(X_{i,j})_{1\le j\le i\le n} \mapsto (X_{i,i-j+1} - i + 2j - 1)_{1\le j\le i\le n}$, corresponding to reflection of bicolored pipe dreams. We say a catalan triangle is *symmetric* if is fixed by this automorphism. Symmetric catalan triangles form a sublattice of $\mathbf{Cat}_n$, whose poset of join-irreducible elements is the vertical half of $\mathcal{J}(\mathbf{Cat}_n)$.

The lattice $\mathbf{Cat}_n$ has an antiautomorphism given by $(X_{i,j})_{1\le j\le i\le n} \mapsto (n+1-X_{i,i-j+1})_{1\le j\le i\le n}$, corresponding to the reflection and exchange of colors of bicolored pipe dreams. We say a catalan triangle is *self-dual* if is fixed by this antiautomorphism.

Table 2 gathers the number of all catalan triangules, of symmetric ones, and of self-dual ones.

n	1	2	3	4	5	6	7	8	9	$\cdots$
$\lvert\mathbf{Cat}_n\rvert$	1	2	6	28	202	2252	38756	1028964	42127054	$\cdots$
symmetric	1	2	4	12	36	168	768	5556	38904	$\cdots$
self-dual	1	0	2	0	10	0	120	0	3434	$\cdots$

TABLE 2. Number of catalan triangles, symmetric catalan triangles and self-dual catalan triangles.

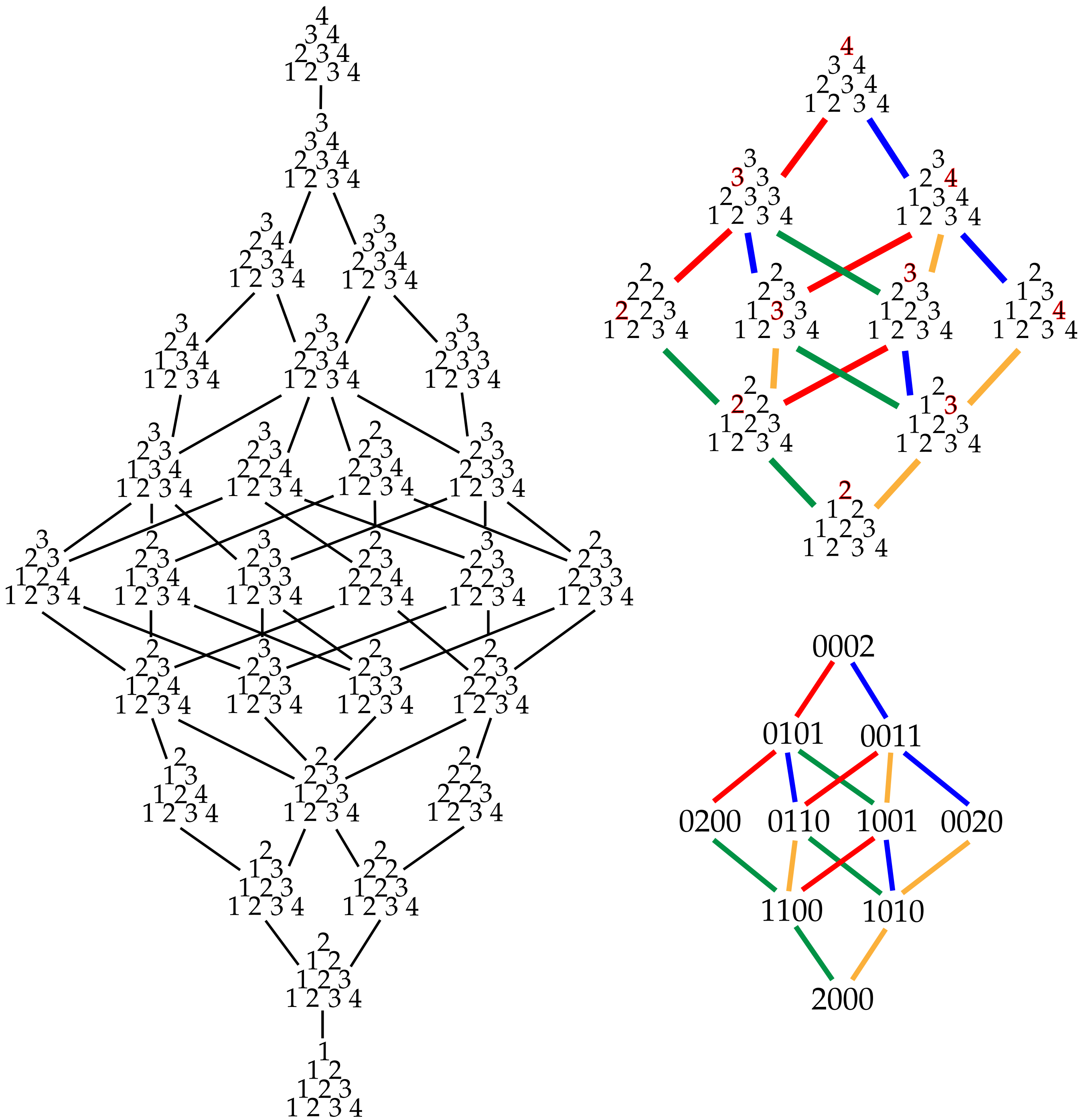

Figure 23. The lattice of catalan triangles of order 5 (left), its join-irreducible poset (top right), and the corresponding barycentric coordinates (bottom right).

5. Maxima of congruence classes

This section is devoted to the maxima of the classes of catalan congruences of $\mathbf{ASM}_n$.

5.1. **Depth antichains.** We first introduce the following objects, motivated by Proposition 4.15 and illustrated in Figure 24.

Definition 5.1. *A depth antichain is a map $\varepsilon : A \to \mathbb{N}$ where A is a (possibly empty) antichain of a triangular poset $\mathcal{D}_n$, such that*

- $-y_2 \le \varepsilon(y_1, y_2, y_3) \le y_2$ *and* $\varepsilon(y_1, y_2, y_3) \equiv_{\text{mod } 2} y_2$ *for all* $(y_1, y_2, y_3) \in A$, *and*
- $|\varepsilon(y_1, y_2, y_3) - \varepsilon(z_1, z_2, z_3)| \le |y_1 - z_1| + |y_3 - z_3|$ *for all* $(y_1, y_2, y_3), (z_1, z_2, z_3) \in A$.

See Figure 24.

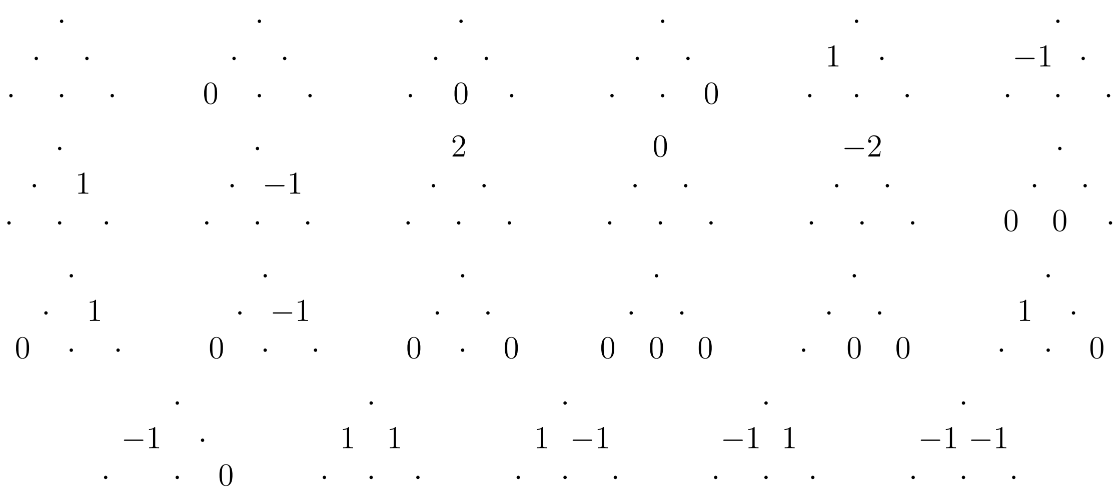

Figure 24. The 23 depth antichains of $\mathcal{D}_4$.

It follows from Proposition 4.11 that the restriction of any depth triangle to any antichain of $\mathcal{D}_n$ is a depth antichain. Conversely, we prove that any depth antichain can be extended to a depth triangle.

Proposition 5.2. *Any depth antichain $\varepsilon : A \to \mathbb{N}$ can be completed into a depth triangle, i.e. there exists a depth triangle $\delta : \mathcal{D}_n \to \mathbb{N}$ which restricts to ε on A.*

To prove Proposition 5.2, we start with depth antichains of size one.

Lemma 5.3. *For any $\boldsymbol{z} := (z_1, z_2, z_3) \in \mathcal{D}_n$ and $-z_2 \le v \le z_2$ with $v \equiv_{\text{mod } 2} z_2$, the map $\delta_{\boldsymbol{z},v} : \mathcal{D}_n \to \mathbb{N}$ defined by $\delta_{\boldsymbol{z},v}(y_1, y_2, y_3) := \min(y_2, v + |y_1 - z_1| + |y_3 - z_3|)$ is a depth triangle with $\delta_{\boldsymbol{z},v}(\boldsymbol{z}) = v$.*

Proof. Since $y_1 + y_2 + y_3 = z_1 + z_2 + z_3$, we have

$$v + |y_1 - z_1| + |y_3 - z_3| \ge v + y_1 - z_1 + y_3 - z_3 \ge -z_2 + y_1 - z_1 + y_3 - z_3 = -y_2.$$

Therefore, we have $-y_2 \le \delta_{\boldsymbol{z},v}(y_1, y_2, y_3) \le y_2$. Hence, the bottom row is indeed $00\cdots0$. Moreover, has $v \equiv_{\text{mod2}} z_2$, we have $y_2 \equiv_{\text{mod } 2} v + |y_1 - z_1| + |y_3 - z_3|$, so that we get that

$$|\delta_{\boldsymbol{z},v}(y_1, y_2, y_3) - \delta_{\boldsymbol{z},v}(y_1, y_2 - 1, y_3 + 1)| = 1 = |\delta_{\boldsymbol{z},v}(y_1, y_2, y_3) - \delta_{\boldsymbol{z},v}(y_1 + 1, y_2 - 1, y_3)|. \qquad \square$$

Lemma 5.4. *For any depth antichain $\varepsilon : A \to \mathbb{N}$, the depth triangle $\delta_\varepsilon : \mathcal{D}_n \to \mathbb{N}$ obtained as the meet (i.e. coordinate-wise minimum) of the depth triangles $\delta_{\boldsymbol{z},\varepsilon(\boldsymbol{z})}$ of Lemma 5.3 for $\boldsymbol{z} \in A$ restricts to ε on A.*

Proof. We have already seen in Remark 4.22 that the coordinate-wise minimum of depth triangles is a depth triangle. Assume by means of contradiction that there is $\boldsymbol{y} \in A$ such that $\delta_\varepsilon(\boldsymbol{y}) \neq \varepsilon(\boldsymbol{y})$. By definition, we have $\delta_{\boldsymbol{y},\varepsilon(\boldsymbol{y})}(\boldsymbol{y}) = \varepsilon(\boldsymbol{y})$. Hence, there is $\boldsymbol{z} \in A$ such that $\delta_{\boldsymbol{z},\varepsilon(\boldsymbol{z})}(\boldsymbol{y}) < \varepsilon(\boldsymbol{y}) \le y_2$. We then get $\varepsilon(\boldsymbol{y}) - \varepsilon(\boldsymbol{z}) > \delta_{\boldsymbol{z},\varepsilon(\boldsymbol{z})}(\boldsymbol{y}) - \varepsilon(\boldsymbol{z}) = |y_1 - z_1| + |y_3 - z_3|$, contradicting the second condition of Definition 5.1. $\square$

Proof of Proposition 5.2. The depth triangle δ_ε of Lemma 5.4 restricts to ε on A. $\square$

5.2. **Covexillary permutations.** Recall that a permutation is vexillary if it avoids the pattern 2143. Here, we are interested in the following variation.

Definition 5.5. *A permutation is covexillary if it avoids the pattern* 3412.

Recall that (i, j) is an ascent of an ASM A if there is another ASM A' such that the corresponding HFMs H, H' satisfy $H'_{i,j} = H_{i,j} + 2$ and $H'_{k,\ell} = H_{k,\ell}$ for all $0 \le k, \ell \le n$ with $(i, j) \neq (k, \ell)$. The following statements are standard. Lemma 5.7 should be intuitively clear from the fact that a -1 in the ASM corresponds to a saddle point in the corresponding surface.

Lemma 5.6. *A permutation is covexillary if and only if it does not have two ascents (i, j) and (k, ℓ) such that $i < k$ and $j > \ell$.*

Lemma 5.7. *If $A_{u,v} = -1$, then*

- *there are $i < u \le k$ and $j < v \le \ell$ such that (i, j) and (k, ℓ) are descents of A,*
- *there are $i < u \le k$ and $j \ge v > \ell$ such that (i, j) and (k, ℓ) are ascents of A.*

For $A \in \mathbf{ASM}_n$, we denote by $\mathrm{m}(A)$ the antichain of $\mathcal{T}_n$ generating the upper set of $\mathcal{T}_n$ corresponding to A, and by $\bar{\mathrm{m}}(A)$ the image of $\mathrm{m}(A)$ under the projection $(x_1, x_2, x_3, x_4) \mapsto (x_1, x_2 + x_3, x_4)$, and by $\varepsilon_A : \bar{\mathrm{m}}(A) \to \mathbb{N}$ the map defined by $\varepsilon_A(x_1, x_2 + x_3, x_4) = x_3 - x_2$ for all $(x_1, x_2, x_3, x_4) \in \mathrm{m}(A)$. Note that ε_A may not be well-defined if the the projection $(x_1, x_2, x_3, x_4) \mapsto (x_1, x_2 + x_3, x_4)$ is not injective from $\mathrm{m}(A)$ to $\bar{\mathrm{m}}(A)$. We are now ready to characterize the maxima of the classes of catalan congruences of $\mathbf{ASM}_n$.

Theorem 5.8. *The following assertions are equivalent for an ASM A of order n:*

(i) A is a covexillary permutation matrix,
(ii) A does not have two ascents (i, j) and (k, ℓ) such that $i < k$ and $j > \ell$,
(iii) ε_A is well-defined and forms a depth antichain of $\mathcal{D}_n$,
(iv) ε_A is well-defined and extends to a depth triangle of order n,
(v) there exists a wall of order n containing $\mathrm{m}(A)$,
(vi) there exists a catalan congruence of $\mathbf{ASM}_n$ such that A is maximal in its class.

Proof. The assertions (i) and (ii) are equivalent by Lemmas 5.6 and 5.7. The assertions (iii) and (iv) are equivalent by Proposition 5.2. The assertions (iv) and (v) are equivalent by Theorem 4.10. The assertions (v) and (vi) are equivalent by (the meet version of) Theorem 4.2 and the definition of walls in connection with Theorem 4.3. We thus just need to prove that the assertions (ii) and (iii) are equivalent.

It follows from the considerations in Sections 2.3 and 4.3 that, when ε_A is well-defined, the following assertions are equivalent for an ASM A and $0 \le i, j \le n$:

- A has an ascent at (i, j),
- there is $(x_1, x_2, x_3, x_4) \in \mathrm{m}(A)$ with $i = x_1 + x_2$ and $j = x_1 + x_3$.
- there is $(y_1, y_2, y_3) \in \bar{\mathrm{m}}(A)$ with $2i = y_1 - y_3 + n - 2 - v$ and $2j = y_1 - y_3 + n - 2 + v$ where $v = \varepsilon_A(y_1, y_2, y_3)$.

Therefore, A has two ascents (i, j) and (k, ℓ) such that $i < k$ and $j > \ell$, if and only if there are $\boldsymbol{y}, \boldsymbol{z} \in \bar{\mathrm{m}}(A)$ with $y_1 - y_3 - \varepsilon_A(\boldsymbol{y}) < z_1 - z_3 - \varepsilon_A(\boldsymbol{z})$ and $y_1 - y_3 + \varepsilon_A(\boldsymbol{y}) > z_1 - z_3 + \varepsilon_A(\boldsymbol{z})$. These two inequalities are equivalent to $\varepsilon_A(\boldsymbol{y}) - \varepsilon_A(\boldsymbol{z}) > |y_1 - z_1 + z_3 - y_3| = |y_1 - z_1| + |y_3 - z_3|$, where the last equality holds since $y_1 < z_1 \iff y_3 > z_3$ as otherwise $\boldsymbol{y}$ and $\boldsymbol{z}$ would be comparable in $\mathcal{D}$. We conclude that the assertions (ii) and (iii) are equivalent. □

Note that conversely, each depth antichain $\varepsilon : A \to \mathbb{N}$ of $\mathcal{D}_n$ defines an ASM A_ε of order $[n]$ obtained as the meet of the meet-irreducible ASMs $m(y_1, (y_2 - v)/2, (y_2 + v)/2, y_3)$ for each $(y_1, y_2, y_3) \in A$ where $v = \varepsilon(y_1, y_2, y_3)$. We thus obtain the following statement.

Corollary 5.9. *The following families are in bijection:*

- *the covexillary permutations of* $[n]$,
- *the depth antichains of* $\mathcal{D}_n$,
- *the ASMs which appear as a maximum of a class in a catalan congruence of* $\mathbf{ASM}_n$.

Example 5.10. *For instance, the* 23 *depth antichains of Figure 24 correspond to the* 23 *covexillary permutations of* $[4]$ *(all except* 3412*).*

Example 5.11. *Following on Example 4.23, consider the congruence corresponding to the minimal (resp. maximum) catalan triangle. Then the maxima of the congruence classes are precisely the permutations avoiding the pattern* 231 *(resp.* 312*). Their mirror permutations are usually called dominant (resp. codominant).*

Remark 5.12. *We conclude by a brief combinatorial description of meet representations of covexillary permutations as these representations are at the heart of this section. Consider a permutation* $\sigma \in \mathfrak{S}_n$*. Draw the permutation matrix* P_σ *(where* $(P_\sigma)_{i,j} = \delta_{\sigma_i, j}$ *for all* $i, j \in [n]$*) and color in red all entries above or to the right of a* 1*, and in green the remaining entries. The green entrees immediately below and to the left of red entries are called the essential points of* σ*. The permutation* σ *is covexillary if and only if no essential point is above and to the right of another essential point (said differently, the green entries form a (broken) Ferrer's shape). Moreover, the canonical meet representation of a covexillary permutation* σ *is given by* $\sigma = \bigwedge_e m(\boldsymbol{x}^e)$ *where* $m(\boldsymbol{x})$ *denotes the anti-bigrassmannian permutation associated to* $\boldsymbol{x} \in \mathcal{T}_n$*, the sum ranges over all essential points* e *of* σ*, and* $\boldsymbol{x}^e := (x^e_1, x^e_2, x^e_3, x^e_4)$ *is the point where*

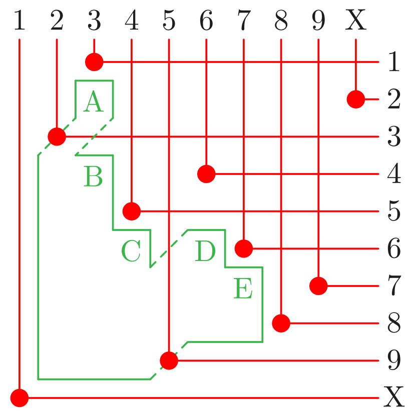

e	A	B	C	D	E
x_1^e	*6*	*5*	*3*	*2*	*1*
x_2^e	*0*	*1*	*2*	*1*	*1*
x_3^e	*2*	*1*	*1*	*2*	*2*
x_4^e	*0*	*1*	*2*	*3*	*4*

FIGURE 25. The matrix of the covexillary permutation $\sigma = 3X26479851$ (left) and the parameters of the anti-bigrassmannian permutations in its canonical meet decomposition (right).

- x_1^e *denotes the number of green entries below* e*,*
- x_2^e *denotes the number of red entries upper right of* e*,*
- x_3^e *denotes the number of red entries to the left of (or equivalently below)* e*,*
- x_4^e *denotes the number of green entries to the left of* e*.*

For instance, Figure 25 illustrates that

$$3X26479851 = m(6,0,2,0) \wedge m(5,1,1,1) \wedge m(3,2,1,2) \wedge m(2,1,2,3) \wedge m(1,1,2,4).$$

As another illustration, note that the permutations avoiding the pattern 231 *from Example 5.11 are precisely those for which the green entries really form a Ferrer's shape in the bottom-left corner of the matrix, and thus whose canonical meetands are of the form* $m(\boldsymbol{x})$ *with* $x_3 = 0$*. A similar characterization of course holds for the permutations avoiding* 312 *by symmetry through the main diagonal, and we obtain canonical meetands are of the form* $m(\boldsymbol{x})$ *with* $x_2 = 0$*.*

6. Minimal permutations of congruence classes

This section is devoted to the minimal permutations in classes of catalan congruences of $\mathbf{ASM}_n$. In contrast to Section 5, the minimum of the congruence classes are not necessarily permutations (see Section 6.3). However, it turns out that each congruence class contains a minimal permutation.

6.1. Nappes.

Recall that for an ASM A, we have denoted by $\mathrm{J}(A)$ the corresponding lower set of the tetrahedron poset $\mathcal{T}_n$.

Definition 6.1. *The nappe of an ASM A of order n is the upper enveloppe of* $\mathrm{J}(A)$*, that is, the set* $\mathrm{N}(A)$ *containing for each* $1 \le i, j \le n$ *the biggest* $(x_1, x_2, x_3, x_4) \in \mathrm{J}(A)$ *such that* $i = x_1 + x_2$ *and* $j = x_1 + x_3$ *(if it exists).*

The following statement is the counterpart of Lemma 4.7. Visually, it states that a nappe cannot enter the interior of the black hourglass illustrated in Figure 27 (middle) at each of its points.

Lemma 6.2. *If (x_1, x_2, x_3, x_4) and (x'_1, x'_2, x'_3, x'_4) are in a nappe, then $x_4 - x'_4$, $x_1 - x'_1$, $x'_3 - x_3$ and $x'_2 - x_2$ cannot be all strictly positive or all strictly negative.*

Proof. Similar to that of Lemma 4.7. □

The following statement asserts that if two permutations $\tau \le \sigma$ differ by a transposition, the lower set $\mathrm{J}(P_\tau)$ can be obtained from the lower set $\mathrm{J}(P_\sigma)$ by removing a rectangular portion of its nappe.

Proposition 6.3. *Let $\sigma, \tau \in \mathfrak{S}_n$ such that $\sigma = \tau \circ (i, j)$ and $\tau < \sigma$. Then*

$$\mathrm{J}(P_\sigma) \smallsetminus \mathrm{J}(P_\tau) = \{(x_1, x_2, x_3, x_4) \in \mathrm{N}(P_\sigma) \mid i \le x_1 + x_2 < j \text{ and } \sigma(j) \le x_1 + x_3 < \sigma(i)\}.$$

We denote this set by $\mathrm{N}_{\sigma,i,j}$.

Proof. We have $\sigma = \tau \circ (i, j)$ with $\tau < \sigma$ if and only if the corresponding corner sum matrices C_σ and C_τ satisfy $(C_\sigma)_{k,\ell} = (C_\tau)_{k,\ell} - 1$ if $i \le k < j$ and $\tau(i) \le \ell < \tau(j)$ and $(C_\sigma)_{k,\ell} = (C_\tau)_{k,\ell}$ otherwise. It follows that $\mathrm{J}(P_\tau)$ can be obtained from $\mathrm{J}(P_\sigma)$ by removing only one join irreducible (x_1, x_2, x_3, x_4) for each value $(x_1 + x_2, x_1 + x_3)$, which must be the biggest. □

Definition 6.4. *Let $\sigma \in \mathfrak{S}_n$ and $i < j$ such that $\sigma \circ (i, j) < \sigma$. We define $P_{\sigma,i,j}$ as the matrix obtained from P_σ by summing rows 1 to $i - 1$, rows $j + 1$ to n, columns 1 to $\sigma(j) - 1$ and columns $\sigma(i) + 1$ to n. See Figure 26.*

$$\begin{pmatrix}
0&1&0&0&0&0&0&0&0&0&0&0&0&0&0\\
0&0&0&0&0&0&0&0&1&0&0&0&0&0&0\\
0&0&0&1&0&0&0&0&0&0&0&0&0&0&0\\
1&0&0&0&0&0&0&0&0&0&0&0&0&0&0\\
0&0&0&0&1&0&0&0&0&0&0&0&0&0&0\\
0&0&0&0&0&0&0&0&0&1&0&0&0&0&0\\
0&0&0&0&0&1&0&0&0&0&0&0&0&0&0\\
0&0&0&0&0&0&0&0&0&0&0&0&0&1&0\\
0&0&0&0&0&0&1&0&0&0&0&0&0&0&0\\
0&0&0&0&0&0&0&0&0&0&0&1&0&0&0\\
0&0&0&0&0&0&0&0&0&0&0&0&1&0&0\\
0&0&0&0&0&0&0&1&0&0&0&0&0&0&0\\
0&0&0&0&0&0&0&0&0&0&1&0&0&0&0\\
0&0&1&0&0&0&0&0&0&0&0&0&0&0&0\\
0&0&0&0&0&0&0&0&0&0&0&0&0&0&1
\end{pmatrix}
\qquad
\begin{pmatrix}
3&0&0&0&0&1&0&0&0&0\\
0&1&0&0&0&0&0&0&0&0\\
0&0&0&0&0&0&1&0&0&0\\
0&0&1&0&0&0&0&0&0&0\\
0&0&0&0&0&0&0&0&0&1\\
0&0&0&1&0&0&0&0&0&0\\
0&0&0&0&0&0&0&0&1&0\\
1&0&0&0&1&0&0&1&0&2
\end{pmatrix}$$

FIGURE 26. Matrices P_σ and $P_{\sigma,i,j}$ with
$\sigma = 2\ 9\ 4\ 1\ 5\ 10\ 6\ 14\ 7\ 12\ 13\ 8\ 11\ 3\ 15$, $i = 5$ and $j = 10$.

Remark 6.5. *When seeing $\mathfrak{S}_n$ as a Coxeter group W generated by the transpositions $s_1 = (1,2), ..., s_{n-1} = (n-1, n)$, the matrices $P_{\sigma,i,j}$ are the contingency matrices corresponding to double cosets in the parabolic quotient $W_I \backslash W / W_J$ where $I = \{s_1, ..., s_{i-2}, s_{j+1}, ..., s_{n-1}\}$ and $J = \{s_1, ..., s_{\sigma(j)-2}, s_{\sigma(i)+1}, ..., s_{n-1}\}$.*

We now show that the matrices $P_{\sigma,i,j}$ where $\sigma \circ (i,j) < \sigma$ are in bijection with the sets of join-irreducibles that are removed from some ideal $\mathrm{J}(P_\sigma)$ when applying a transposition (i,j) to P_σ.

Proposition 6.6. *Let $\sigma_1 \in \mathfrak{S}_n$ and $i_1 < j_1$ such that $\sigma_1 \circ (i_1, j_1) < \sigma_1$, and $\sigma_2 \in \mathfrak{S}_n$ and $i_2 < j_2$ such that $\sigma_2 \circ (i_2, j_2) < \sigma_2$. Then $\mathrm{N}_{\sigma_1,i_1,j_1} = \mathrm{N}_{\sigma_2,i_2,j_2}$ if and only if $i_1 = i_2$, $j_1 = j_2$ and $P_{\sigma_1,i_1,j_1} = P_{\sigma_2,i_2,j_2}$.*

Proof. By Proposition 6.3, $\mathrm{N}_{\sigma,i,j}$ is the set of join-irreducible elements in $\mathrm{J}(P_\sigma) \smallsetminus \mathrm{J}(P_\tau)$ where $\sigma = \tau \circ (i,j)$. The elements of the nappe of an ASM correspond to the values and positions of the entries of its height function. Hence $\mathrm{N}_{\sigma_1,i_1,j_1} = \mathrm{N}_{\sigma_2,i_2,j_2}$ if and only if the height functions of P_{σ_1} and P_{σ_2} have the same values in the rectangle between rows $i_1 = i_2$ to $j_1 = j_2$ and columns $\sigma(j_1)$ to $\sigma(i_1)$, which is equivalent to $P_{\sigma_1,i_1,j_1} = P_{\sigma_2,i_2,j_2}$. ☐

Finally, we exploit Proposition 6.6 to count the distinct sets of the form $N_{\sigma,i,j}$, and those corresponding to cover relations in the Bruhat order. The first few values of these numbers are gathered in Table 3.

n	1	2	3	4	5	6	7	8	9	10	$\cdots$
N_n	0	1	9	52	260	1291	6915	41814	289758	2291381	$\cdots$
O_n	0	1	8	38	140	443	1268	3384	8584	20965	$\cdots$

TABLE 3. First values of N_n and O_n from Proposition 6.7. Note that O_n is [OEI10, A034009].

Proposition 6.7. *The ordinary generating function of the number N_n of distinct sets of the form $N_{\sigma,i,j}$ with $\sigma \in \mathfrak{S}_n$ is given by*

$$\sum_{n \geq 1} N_n x^n = \frac{x^2}{(1-x)^4} \sum_{a,b,c,d,e \geq 0} \frac{(a+b+c)!\ (a+d+e)!}{a!\ b!\ c!\ d!\ e!} x^{a+b+c+d+e}.$$

The ordinary generating function of the number O_n of these sets which correspond to cover relations in the Bruhat order is given by

$$\sum_{n \geq 1} O_n x^n = \frac{x^2}{(1-x)^4(1-2x)^2}.$$

Proof. Matrix of the form $P_{\sigma,i,j}$ are made of a permutation matrix shuffled with entries equal to 1 on its four sides, the two entries exchanged by the transposition (i,j), and four integers in the corners (see Figure 26 for an illustration). These matrices can be enumerated by distinguishing them according to the size of the permutation matrix in the middle and the number of 1 entries on each side. The matrices corresponding to cover relations are those with an empty permutation matrix in the middle. ☐

6.2. **Minimal permutations.** We are now ready to describe the minimal permutations in the classes of a catalan congruence of $\mathbf{ASM}_n$. The following statement follows from Lemmas 4.7 and 6.2. Visually, it states that the intersection of a wall and a nappe must remain in the complement of the butterfly and of the hourglass at each of its points, which is illustrated in green in Figure 27 (right).

Lemma 6.8. *If* N *is the nappe of an ASM, and* $\mathcal{P}$ *is a wall of a congruence, and if* (x_1, x_2, x_3, x_4) *and* (x_1', x_2', x_3', x_4') *are both in* $\mathrm{N} \cap \mathcal{P}$*, then* $x_1 + x_2 - x_1' - x_2'$*,* $x_1 + x_3 - x_1' - x_3'$*,* $x_4' - x_4$ *and* $x_1 - x_1'$ *are all positive or all negative.*

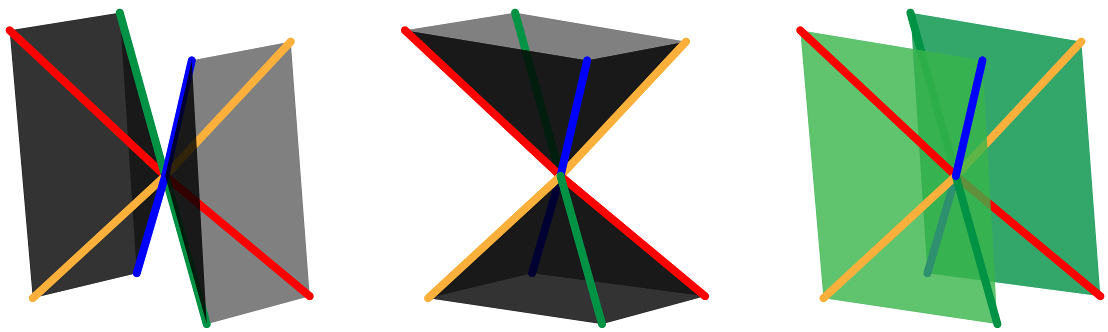

FIGURE 27. The butterfly (left), the hourglass (middle), and the complement of their union (right).

Proposition 6.9. *Let* $\equiv$ *be a catalan congruence of* $\mathbf{ASM}_n$*. Let* $\sigma \in \mathfrak{S}_n$ *containing the pattern* 321*, and let* $i < j < k$ *be such that* $\sigma(i) > \sigma(j) > \sigma(k)$*. Then at least one of the permutations* $\sigma \circ (i, j)$ *and* $\sigma \circ (j, k)$ *is congruent to* σ*. Moreover, if both are, then* $\sigma \circ (i, k)$ *is also congruent to* σ*.*

Proof. We show that at least one of the permutations $\sigma \circ (i, j)$ and $\sigma \circ (j, k)$ is congruent to σ. Let $\mathcal{P}$ be the wall inducing $\equiv$, *i.e.* the corresponding subposet of $\mathcal{T}_n$ isomorphic to $\mathcal{D}_n$. Suppose $\sigma \circ (i, j)$ is not congruent to σ. By Proposition 6.3, this is equivalent to $\mathcal{P}$ intersecting $\mathrm{N}_{\sigma,i,j}$. By Lemma 6.8, if (x_1, x_2, x_3, x_4) and (y_1, y_2, y_3, y_4) are in $\mathrm{N}_{\sigma,i,j} \cap \mathcal{P}$, then $x_1 + x_2 - y_1 - y_2$, $x_1 + x_3 - y_1 - y_3$ are both positive or both negative. This implies that if $(x_1, x_2, x_3, x_4) \in \mathrm{N}_{\sigma,i,j}$, $\mathcal{P}$ cannot intersect $\mathrm{N}_{\sigma,j,k}$ (since (y_1, y_2, y_3, y_4) must be in the shaded area of Figure 28 (a)), hence $\sigma \circ (j, k)$ is congruent to σ.

We now prove that if both permutations $\sigma \circ (i, j)$ and $\sigma \circ (j, k)$ are congruent to σ, then $\sigma \circ (i, k)$ is also congruent to σ. For this, suppose that $(x_1, x_2, x_3, x_4) \in \mathrm{N}_{\sigma,i,k} \cap \mathcal{P}$. We can assume without loss of generality that (x_1, x_2, x_3, x_4) is in the bottom left corner, *i.e.* $x_1 + x_3 + 1 \geq j$ and $x_1 + x_2 + 1 < \sigma(j)$. It is possible to find elements of $\mathrm{N}_{\sigma,i,k} \cap \mathcal{P}$ closer to $\mathrm{N}_{\sigma,i,j}$ or $\mathrm{N}_{\sigma,j,k}$, until we eventually reach it: if $(x_1, x_2, x_3 + 1, x_4 - 1)$, $(x_1, x_2 + 1, x_3, x_4 - 1)$, $(x_1 + 1, x_2, x_3 - 1, x_4)$ and $(x_1 + 1, x_2 - 1, x_3, x_4)$ are not in $\mathrm{N}_{\sigma,i,k} \cap \mathcal{P}$, then $(x_1 + 1, x_2, x_3, x_4 - 1)$ is in $\mathrm{N}_{\sigma,i,k} \cap \mathcal{P}$, and this can only be the case if the two elements of the nappe to the right and above (x_1, x_2, x_3, x_4) have different heights (value of $x_2 + x_3$). Hence we cannot go between $\mathrm{N}_{\sigma,i,j}$ and $\mathrm{N}_{\sigma,j,k}$ without intersecting one of them, since there is a entry equal to 1 there which corresponds to a saddle point in the nappe (cf. Figure 28 (b)). □

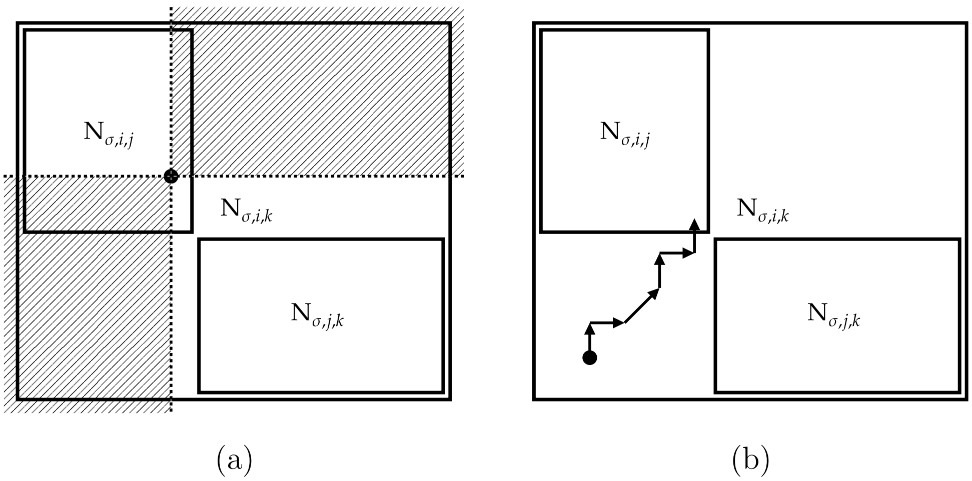

FIGURE 28. The nappes $\mathrm{N}_{\sigma,i,j}$, $\mathrm{N}_{\sigma,j,k}$ and $\mathrm{N}_{\sigma,i,k}$ of Proposition 6.9.

Theorem 6.10. *For a catalan congruence of* $\mathbf{ASM}_n$*,*

- *each congruence class contains a unique minimal permutation,*
- *the minimal permutations of the congruence classes are precisely the* 321*-avoiding permutations.*

Proof. By Proposition 6.9, a permutation containing the pattern 321 cannot be minimal in its congruence class. By Theorem 5.8, each class contains a permutation, hence at least one minimal permutation, which must avoid 321 by Proposition 6.9. The result follows since the number of 321-avoiding permutations is the same as the number of elements of $\mathbf{Dyck}_n$. □

6.3. **Minimal elements versus minimal permutations.** We say that an ASM is *permutational* if it is the matrix P_σ of a permutation σ, and *non-permutational* otherwise. As already mentioned, the minimal (and maximal) ASMs of the classes of a congruence of $\mathbf{ASM}_n$ are not necessarily permutational. Surprisingly, we have seen in Theorem 5.8 that the maxima are permutational for the specific congruences of $\mathbf{ASM}_n$ considered in this paper. We will now observe that the minima for these specific congruences are not all permutational as soon as $n \geq 3$ (as illustrated in Figure 13).

Recall that for an ASM A, we denote by $\mathrm{J}(A)$ the corresponding lower set of $\mathcal{T}_n$, and by $\mathrm{j}(A)$ the antichain of $\mathcal{T}_n$ generating $\mathrm{J}(A)$. Recall also from Theorem 4.2 that for a congruence $\equiv$ of $\mathbf{ASM}_n$ with non-contracted join irreducibles $\mathcal{J}(\equiv) \subseteq \mathcal{T}_n$, the minima of the congruence classes are precisely the ASMs A such that $\mathrm{j}(A) \subseteq \mathcal{J}(\equiv)$. This directly yields the following statement.

Corollary 6.11. *The following conditions are equivalent for a lattice congruence $\equiv$ of $\mathbf{ASM}_n$:*

- *the minima of the congruence classes of $\equiv$ are all permutational,*
- $\mathrm{j}(A) \nsubseteq \mathcal{J}(\equiv)$ *for each non-permutational ASM A,*
- $\mathcal{J}(\mathbf{ASM}_n) \smallsetminus \mathcal{J}(\equiv)$ *is a transversal of the set $\{\mathrm{j}(A) \mid A$ non-permutational ASM$\}$.*

This immediately yields the following.

Corollary 6.12. *For $n \geq 3$ and any catalan congruence $\equiv$ of $\mathbf{ASM}_n$, there is at least one congruence class of $\equiv$ whose minima is non-permutational.*

Proof. As $\equiv$ is a catalan congruence, both $j(0,0,0,n-2)$ and $j(1,0,0,n-3)$ belong to $\mathcal{J}(\equiv)$ by Proposition 4.4, and $j(0,0,0,n-2) \vee j(1,0,0,n-3)$ has a -1 in position $(2,2)$. □

We now show that the condition of Corollary 6.11 can be largely simplified using the following lemma.

Lemma 6.13. *For any non-permutational ASM A, there exists a non-permutational ASM A' such that $|\,\mathrm{j}(A')| = 2$ and $\mathrm{j}(A') \subseteq \mathrm{j}(A)$.*

Proof. We have seen in Section 2.3 that the 1 and -1 entries in an ASM corresponds to the saddle points in the corresponding surface. More precisely, for any $x_1, x_2, x_3, x_4 \in \mathbb{N}$, the ASM A has a -1 in position $(x_1 + x_2 + 1, x_1 + x_3 + 1)$ if and only if $\mathrm{J}(A)$ contains both $j_1 := j(x_1+1, x_2, x_3, x_4)$ and $j_4 := j(x_1, x_2, x_3, x_4+1)$ but neither $j_2 := j(x_1, x_2+1, x_3, x_4)$ nor $j_3 := j(x_1, x_2, x_3+1, x_4)$. The latter happens if and only if $\mathrm{j}(A)$ contains two join irreducibles J, J' such that $j_1 \leq J$ and $j_4 \leq J'$ but neither J nor J' is larger than j_2 nor j_3. We conclude that $A' = J \vee J'$ also contains a -1 at the same position as A. □

Corollary 6.14. *The following conditions are equivalent for a lattice congruence $\equiv$ of $\mathbf{ASM}_n$:*

- *the minima of the congruence classes of $\equiv$ are all permutational,*
- $\mathrm{j}(A) \nsubseteq \mathcal{J}(\equiv)$ *for each non-permutational ASM A with $|\,\mathrm{j}(A)| = 2$,*
- $\mathcal{J}(\mathbf{ASM}_n) \smallsetminus \mathcal{J}(\equiv)$ *is a vertex cover of the graph on $\mathcal{J}(\mathbf{ASM}_n)$ with an edge $\{J, J'\}$ if and only if $J \vee J'$ is non-permutational.*

Of course, there is a dual statement for all maxima to be permutational. For completeness, we note that the same arguments enable to prove the following version, considering simultaneously minima and maxima.

Corollary 6.15. *The following conditions are equivalent for a lattice congruence $\equiv$ of $\mathbf{ASM}_n$:*

- *the minima and maxima of the congruence classes of $\equiv$ are all permutational,*
- $\mathcal{J}(\mathbf{ASM}_n) \smallsetminus \mathcal{J}(\equiv)$ *is a vertex cover of the graph on $\mathcal{J}(\mathbf{ASM}_n)$ with an edge $\{J, J'\}$ if and only if $J \vee J'$ or $\kappa(J) \wedge \kappa(J')$ is non-permutational.*

Corollaries 6.14 and 6.15 turns the enumeration of lattice congruences of $\mathbf{ASM}_n$ where minima and/or maxima are required to be permutational into an enumeration of vertex covers. Table 4 gathers the first few values.

n	2	3	4	5	6	7	$\cdots$
all congruences	2	16	1024	1048576	34359738368	72057594037927936	$\cdots$
min permutational	2	12	216	10480	1344096	465473984	$\cdots$
min and max permutational	2	9	69	716	8986	128065	$\cdots$

Table 4. The numbers of congruences of $\mathbf{ASM}_n$ depending on whether we require all minima and/or maxima to be permutational. Note that the first line is [OEI10, A125791]

7. Bases of the Temperley–Lieb algebra

In this section, we construct various bases of the Temperley–Lieb algebra $\mathrm{TL}_n(2)$ using the quotients studied in Sections 4 to 6, following the work of [BG24].

7.1. The Temperley–Lieb algebra. Recall that, for $q \in \mathbb{C}$, the *Temperley–Lieb algebra* $\mathrm{TL}_n(q)$ is the $\mathbb{C}$-algebra generated by $e_1, \dots, e_{n-1}$ subject to the *Jones relations*

- $e_i^2 = qe_i$ for $i \in [n-1]$,
- $e_ie_{i+1}e_i = e_i$ for $i \in [n-2]$,
- $e_{i+1}e_ie_{i+1} = e_{i+1}$ for $i \in [n-2]$,
- $e_ie_j = e_je_i$ for $i, j \in [n-1]$ with $|i-j| \neq 1$.

Although we will not use it in this paper, let us recall that there is also a classical diagrammatic description of $\mathrm{TL}_n(q)$ as the vector space generated by noncrossing matchings of two vertical lines of n points, where the multiplication of two diagrams is obtained by concatenating them and replacing each closed loop by a factor q, and where the generator e_i corresponds to the diagram connecting the ith and $(i+1)$th points of each line, and the jth points of both lines for all $j \notin \{i, i+1\}$. See Figure 29.

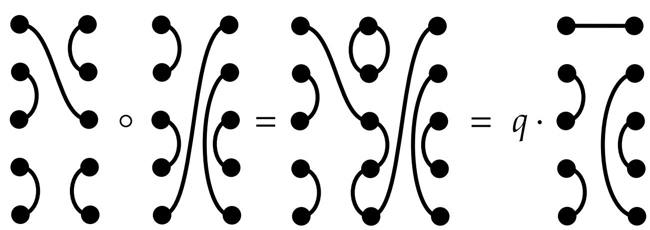

Figure 29. The classical diagrammatic description of the Temperley–Lieb algebra.

7.2. Bases. In this section, we produce various bases of the Temperley–Lieb algebra $\mathrm{TL}_n(2)$ following [BG24]. It is well known that

$$\mathrm{TL}_n(2) \simeq \mathbb{C}\mathfrak{S}_n / \left\langle () - (ij) - (jk) - (ik) + (ijk) + (ikj) \mid 1 \le i < j < k \le n \right\rangle,$$

where permutations are written in cycle notation. Hence any 321 pattern can be rewritten as $321 \to 123 - 213 - 132 + 231 + 312$. As a consequence, the set T_n of 321-avoiding permutations of $[n]$ forms a basis of $\mathrm{TL}_n(2)$. This was extended in [BG24] to the following.

Theorem 7.1 ([BG24])**.** *Any choice of representative permutations of the excedance classes on $\mathfrak{S}_n$ forms a basis of the Temperley–Lieb algebra $\mathrm{TL}_n(2)$.*

We extend this result to all catalan congruences of $\mathbf{ASM}_n$.

Theorem 7.2. *Any choice of representative permutations in the classes of any catalan congruence $\equiv$ of $\mathbf{ASM}_n$ forms a basis of $\mathrm{TL}_n(2)$.*

Proof. Using the relation $(ik) = () - (ij) - (jk) + (ijk) + (ikj)$, we obtain that any permutation $\sigma \in \mathfrak{S}_n$ can be written as a linear combination of permutations avoiding 321 that are below σ in the Bruhat order

$$\sigma = \sum_{\tau \in T_n, \tau \leq \sigma} c_{\tau,\sigma}\ \tau.$$

By Theorem 6.10, the congruence class of σ contains a unique minimal permutation τ, which moreover avoids the pattern 321. We prove by induction that $c_{\tau,\sigma} = 1$. This is obvious if $\sigma = \tau$, *i.e.* if σ avoids the pattern 321. Assume now that $\tau < \sigma$ and suppose by induction that $c_{\tau,\sigma'} = 1$ for any permutations σ' such that $\tau \leq \sigma' < \sigma$. Note that for $\sigma' < \sigma$, we have $\tau \leq \sigma'$ if and only if $\sigma' \equiv \sigma$. Since $\sigma \neq \tau$, there is $i < j < k$ such that $\sigma(i) > \sigma(j) > \sigma(k)$, so that $\sigma = \sigma\circ(i,j) + \sigma\circ(j,k) - \sigma\circ(i,j,k) - \sigma\circ(i,k,j) + \sigma\circ(i,k)$. Proposition 6.9 states that at least one of the permutations $\sigma\circ(i,j)$ and $\sigma\circ(j,k)$ is congruent to σ. If only $\sigma\circ(i,j)$ is congruent to σ, then we get $c_{\tau,\sigma} = c_{\tau,\sigma\circ(i,j)} = 1$ since all the other permutations in the relation are not congruent to σ, hence not larger than τ. If both $\sigma\circ(i,j)$ and $\sigma\circ(j,k)$ are congruent to σ, then $\sigma\circ(i,j,k)$, $\sigma\circ(i,k,j)$, and $\sigma\circ(i,k)$ are also congruent to them and we get $c_{\tau,\sigma} = c_{\tau,\sigma\circ(i,j)} + c_{\tau,\sigma\circ(j,k)} - c_{\tau,\sigma\circ(i,j,k)} - c_{\tau,\sigma\circ(i,k,j)} + c_{\tau,\sigma\circ(i,k)} = 1$. By triangularity, any set of representatives of the congruence classes of $\equiv$ can be expressed as linearly independent combinations of the 321-avoiding permutations, hence forms a basis of $\mathrm{TL}_n(2)$. ☐

8. Posets $\mathcal{P}^n/\mathfrak{S}_n$

To conclude this paper, we observe that the join irreducible posets of all the lattices considered along the paper (and many others) are all instances of a general symmetrization operation on posets, which will certainly deserve further study.

Let $\mathcal{P}$ be a finite poset and $n \geq 0$. The set $\mathcal{P}^n$ of n-tuples of elements of $\mathcal{P}$ is ordered by coordinatewise comparison. For all $\boldsymbol{x} = (x_1, \dots, x_n) \in \mathcal{P}^n$ and $\sigma \in \mathfrak{S}_n$, we write $\boldsymbol{x}^\sigma := (x_{\sigma(1)}, \dots, x_{\sigma(n)})$. We consider the set $\mathcal{P}^n/\mathfrak{S}_n$ of tuples of $\mathcal{P}^n$ up to permutation of their coordinates. We write $\bar{\boldsymbol{x}} \leq \bar{\boldsymbol{y}}$ if there exists $\boldsymbol{x} \in \bar{\boldsymbol{x}}$ and $\boldsymbol{y} \in \bar{\boldsymbol{y}}$ such that $\boldsymbol{x} \leq \boldsymbol{y}$.

Proposition 8.1. *The relation $\leq$ is a partial order on $\mathcal{P}^n/\mathfrak{S}_n$.*

Proof. The relation $\equiv$ is

- reflexive since $\boldsymbol{x} \leq \boldsymbol{x}$ for any $\boldsymbol{x} \in \bar{\boldsymbol{x}}$,
- transitive since $\boldsymbol{x} \leq \boldsymbol{y}^\sigma$ and $\boldsymbol{y} \leq \boldsymbol{z}^\tau$ implies $\boldsymbol{x} \leq \boldsymbol{z}^{\tau\sigma}$,
- antisymmetric since $\boldsymbol{x} \leq \boldsymbol{x}^\sigma$ implies that $\boldsymbol{x}$ is constant on every cycle of σ (since $x_{i_1} \leq x_{\sigma(i_1)} = x_{i_2} \leq \cdots \leq x_{i_k} \leq x_{\sigma(i_k)} = x_{i_1}$ for any cycle $(i_1, \dots, i_k)$ of σ), hence that $\boldsymbol{x} = \boldsymbol{x}^\sigma$. ☐

Example 8.2. *For the 2-element chain $\mathcal{C}_2$, the poset $\mathcal{C}_2^n$ is the boolean lattice, and the quotient $\mathcal{C}_2^n/\mathfrak{S}_n$ is a $(n+1)$-element chain. For the k-element chain $\mathcal{C}_k$, the poset $\mathcal{C}_k^n$ is a poset on the integer points in the $(k-1)$th dilate of the cube, and $\mathcal{C}_k^n/\mathfrak{S}_n$ is a poset on the integer points in one of the fundamental simplices of this cube.*

Example 8.3. *As illustrated in Figure 30, the join irreducible posets of the lattices $\mathbf{ASM}_n$, $\mathbf{Dyck}_n$ and $\mathbf{Cat}_n$ considered in this paper are all instances of Proposition 8.1. Other examples include the join irreducible posets of the lattices of totally symmetric partitions, Magog triangles, gapless triangles, Gelfand-Tsetlin triangles with top line $12\cdots n$,* etc.

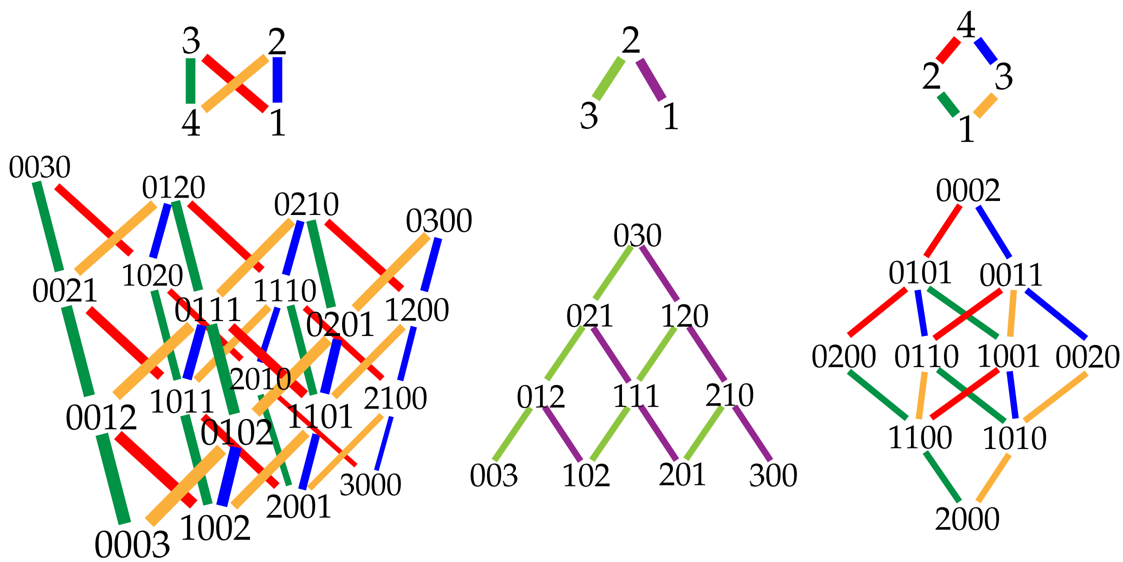

FIGURE 30. The posets $\mathcal{P}$ (top) such that $\mathcal{P}^{n-2}/\mathfrak{S}_{n-2}$ (bottom) is isomorphic to the join irreducible posets of $\mathbf{Dyck}_n$ (left), $\mathbf{ASM}_n$ (middle) and $\mathbf{Cat}_n$ (right). Here, $n = 3$ for the first two columns, and $n = 2$ for the last one.

An element $\bar{\boldsymbol{x}} \in \mathcal{P}^n/\mathfrak{S}_n$ can be encoded by the vector $(|\boldsymbol{x}|_p)_{p\in\mathcal{P}}$ where $|\boldsymbol{x}|_p$ denotes the number of occurences of p in any representative $\boldsymbol{x} \in \bar{\boldsymbol{x}}$. These vectors generalize the barycentric coordinates described earlier to encode the join irreducible ASMs, Dyck paths, and Catalan triangles.

Proposition 8.4. *The following assertions are equivalent for any $\boldsymbol{x}, \boldsymbol{y} \in \mathcal{P}^n$:*

(i) $\bar{\boldsymbol{x}} \le \bar{\boldsymbol{y}}$, *i.e. there exists $\sigma \in \mathfrak{S}_n$ such that $\boldsymbol{x} \le \boldsymbol{y}^\sigma$ componentwise,*
(ii) $\sum_{p\in U} |\boldsymbol{x}|_p \le \sum_{p\in U} |\mathbf{y}|_p$ *for all upper sets U of $\mathcal{P}$,*
(iii) there exists a nonnegative flow on the Hasse diagram of $\mathcal{P}$ with excess function $p \mapsto |\boldsymbol{x}|_p - |\mathbf{y}|_p$.

Proof. (i) $\Rightarrow$ (iii): Let σ be such that $\boldsymbol{x} \le \boldsymbol{y}^\sigma$ componentwise. For each $i \in [n]$, let f_i denote the flow on the Hasse diagram of $\mathcal{P}$ with 1 along an arbitrary directed path joining x_i

to $y_{\sigma^{-1}(i)}$ and 0 elsewhere. Then $\sum_{i\in[n]} f_i$ is a nonnegative flow on the Hasse diagram of $\mathcal{P}$ with excess function $p \mapsto |\boldsymbol{x}|_p - |\mathbf{y}|_p$.

(iii) $\Rightarrow$ (ii): Consider a nonnegative flow f on the Hasse diagram of $\mathcal{P}$ with excess function $p \mapsto |\boldsymbol{x}|_p - |\mathbf{y}|_p$ and let U be an upper set of $\mathcal{P}$. Then $\sum_{p\in U} |\boldsymbol{x}|_p - |\mathbf{y}|_p$ equals the incoming flow of f to U, hence it is nonnegative.

(ii) $\Rightarrow$ (i): Assume that $\sum_{p\in U} |\boldsymbol{x}|_p \leq \sum_{p\in U} |\mathbf{y}|_p$ for all upper sets U of $\mathcal{P}$. Consider the the bipartite graph $G \coloneqq (X \sqcup Y, E)$ where $X \coloneqq \{(p,k) \mid p \in \mathcal{P} \text{ and } 1 \leq k \leq |\boldsymbol{x}|_p\}$ while $Y \coloneqq \{(p,k) \mid p \in \mathcal{P} \text{ and } 1 \leq k \leq |\boldsymbol{y}|_p\}$, and E has an edge between $(p_1,k_1) \in X$ and $(p_2,k_2) \in Y$ if and only if $p_1 \leq p_2$. Consider an arbitrary subset $W \subseteq X$, denote by $N_G(W) \coloneqq \bigcup_{x\in W} \{y \in Y \mid (x,y) \in E\}$ the neighborhood of W in G, and by U the upper set of $\mathcal{P}$ generated by elements $p \in \mathcal{P}$ such that there exists some $(p,i) \in W$. Then

$$|W| \leq \sum_{p\in U} |\boldsymbol{x}|_p \leq \sum_{p\in U} |\boldsymbol{y}|_p = |N_G(W)|,$$

where the second inequality holds by (ii). Hence, by application of Hall's perfect matching theorem, there is a matching of G covering X. This matching clearly defines a permutation $\sigma \in \mathfrak{S}_n$ with $\boldsymbol{x} \leq \boldsymbol{y}^\sigma$. $\square$

Acknowledgments

We are grateful to Lucas Gagnon, Jean-Christophe Novelli, and Wenjie Fang for their insightful discussions and suggestions. We also thank Romain Di Vozzo for his helpful discussions and assistance with the 3D models.

References

[AB03] J.-C. Aval and N. Bergeron. Catalan paths and quasi-symmetric functions. *Proc. Amer. Math. Soc.*, 131(4):1053–1062, 2003.

[ACGB11] Arvind Ayyer, Robert Cori, and Dominique Gouyou-Beauchamps. Monotone triangles and 312 pattern avoidance. *Electron. J. Combin.*, 18(2):Paper 26, 22, 2011.

[BB93] Nantel Bergeron and Sara Billey. RC-graphs and Schubert polynomials. *Experiment. Math.*, 2(4):257–269, 1993.

[BG24] Nantel Bergeron and Lucas Gagnon. The excedance quotient of the Bruhat order, quasisymmetric varieties, and Temperley-Lieb algebras. *J. Lond. Math. Soc. (2)*, 110(4):Paper No. e13007, 28, 2024.

[Ges84] Ira M. Gessel. Multipartite P-partitions and inner products of skew Schur functions. In *Combinatorics and algebra (Boulder, Colo., 1983)*, volume 34 of *Contemp. Math.*, pages 289–317. Amer. Math. Soc., Providence, RI, 1984.

[GH93] Adriano M. Garsia and Mark Haiman. A graded representation model for Macdonald's polynomials. *Proc. Nat. Acad. Sci. U.S.A.*, 90(8):3607–3610, 1993.

[GW16] Thomas Gobet and Nathan Williams. Noncrossing partitions and Bruhat order. *European J. Combin.*, 53:8–34, 2016.

[Hai01] Mark Haiman. Hilbert schemes, polygraphs and the Macdonald positivity conjecture. *J. Amer. Math. Soc.*, 14(4):941–1006, 2001.

[Hiv00] Florent Hivert. Hecke algebras, difference operators, and quasi-symmetric functions. *Adv. Math.*, 155(2):181–238, 2000.

[KM05] Allen Knutson and Ezra Miller. Gröbner geometry of Schubert polynomials. *Ann. of Math. (2)*, 161(3):1245–1318, 2005.

[KT97] Daniel Krob and Jean-Yves Thibon. Noncommutative symmetric functions. IV. Quantum linear groups and Hecke algebras at $q = 0$. *J. Algebraic Combin.*, 6(4):339–376, 1997.

[LS87] Alain Lascoux and Marcel-Paul Schützenberger. Symmetrization operators in polynomial rings. *Functional Analysis*, 21(4):77–78, 1987.

[Mac91] I. G. Macdonald. Schubert polynomials. In *Surveys in combinatorics, 1991 (Guildford, 1991)*, volume 166 of *London Math. Soc. Lecture Note Ser.*, pages 73–99. Cambridge Univ. Press, Cambridge, 1991.

[OEI10] The On-Line Encyclopedia of Integer Sequences. Published electronically at http://oeis.org, 2010.

[Pro01] James Propp. The many faces of alternating-sign matrices. In *Discrete models: combinatorics, computation, and geometry (Paris, 2001)*, Discrete Math. Theor. Comput. Sci. Proc., AA, pages 043–058. Maison Inform. Math. Discrèt. (MIMD), Paris, 2001.

[Str11] Jessica Striker. A unifying poset perspective on alternating sign matrices, plane partitions, Catalan objects, tournaments, and tableaux. *Adv. in Appl. Math.*, 46(1-4):583–609, 2011.

[Thu54] A. H. Thurston. Congruences on a distributive lattice. *Proc. Edinburgh Math. Soc. (2)*, 10:76–77, 1954.

[Zin02] Matthew G. Zinno. A Temperley-Lieb basis coming from the braid group. volume 11, pages 575–599. 2002. Knots 2000 Korea, Vol. 2 (Yongpyong).

(Florent Hivert) LRI, Université Paris-Sud, Orsay
Email address: florent.hivert@lri.fr
URL: http://www.lri.fr/~hivert/

(Vincent Pilaud) Universitat de Barcelona & Centre de Recerca Matemàtica, Barcelona
Email address: vincent.pilaud@ub.edu
URL: https://www.ub.edu/comb/vincentpilaud/

(Ludovic Schwob) LIGM, Université Gustave Eiffel, Champs-sur-Marne
Email address: ludovic.schwob@edu.univ-eiffel.fr
URL: https://igm.univ-mlv.fr/~schwob/